NATIONAL ADVISORY COMMITTEE FOR AERONAUTICS

WARTIME REPORT

ORIGINALLY ISSUED
August 1941 as
Memorandum Report

STATIC CHARACTERISTICS OF CURTISS PROPELLERS HAVING DIFFERENT BLADE SECTIONS

By Blake W. Corson, Jr., and Nicholas Mastrocola

Langley Memorial Aeronautical Laboratory
Langley Field, Va.

NACA

WASHINGTON

MEMORANDUM REPORT

for

Army Air Corps

STATIC CHARACTERISTICS OF CURTISS PROPELLERS HAVING DIFFERENT BLADE SECTIONS

By BLAKE W. CORSON, JR., and NICHOLAS MASTROCOLA

SUMMARY

Static tests were made on four full-scale two-bladed propellers differing only in blade sections, at blade angles from 0° to 20° at the three-quarters radius. Two of the same propellers were tested as three bladed propellers. The tests were made outdoors under conditions of low wind velocity.

The data are analyzed on the basis of a static thrust figure of merit and by Driggs Simplified Propeller Calculations, which is a single-point method of reducing propeller data to airfoil data. Static propeller data are reduced to airfoil data for all of the propellers tested. These airfoil data for the two three bladed propellers have been reconverted to propeller efficiency as a function of advance ratio for the purpose of comparing the modified NACA 16-series blade sections with the Clark Y blade section.

The propeller with Clark Y blade sections yields slightly higher efficiency in take-off and climb than the modified 16-series sections. The propeller with modified 16-series sections may yield efficiencies higher by 2 or 3 percent than a similar propeller with Clark Y sections

at the high speeds now attainable by some airplanes. The double cambered Clark Y gives only slightly lower efficiency than the modified 16-series section for high speed and slightly higher efficiencies for take-off. A slight increase in the radii of the leading and trailing edges of the modified 16-series sections has little effect on the behavior of the sections.

INTRODUCTION

The tests described in this report constitute one phase of an investigation described in reference 1 to check flight tests made for the purpose of determining the relative merits of the Clark Y and a modified 16-series section. The tests were made on propellers operating at zero forward velocity. Thrust and power were measured at various propeller tip speeds and blade angle settings. The propeller blades used were Curtiss blades identical in all respects except blade sections. One set of blades had Clark Y sections, another set was made with double cambered Clark Y sections, and a third set embodied modified NACA 16-series sections. The investigation included tests both on two bladed and three bladed propellers.

As the static test conditions can not be universally representative of conditions of application, the absolute values obtained from these tests are not highly significant. The results, however, can be very useful for making qualitative comparisons of propellers tested under identical conditions.

The purpose of this investigation was to determine the relative merits of the Clark Y, double cambered Clark Y, and NACA 16-series propeller sections under varied loading and at various tip speeds. The propellers are compared on the basis of a static thrust figure of merit. As a further analysis, use is made of Driggs Simplified Propeller Calculations, reference 2, for reducing the propeller characteristics to quasi airfoil characteristics. The airfoil polars so obtained were then reconverted into the propeller envelope efficiency as a function of the advance ratio, for two of the propellers.

This investigation was made at the request of the Army Air Corps, War Department. The testing was done on the static test equipment of the propeller-research section of the National Advisory Committee for Aeronautics at Langley Field, Virginia.

DESCRIPTION OF APPARATUS

Test rig.- The static propeller-test rig used in this investigation, located outdoors, was essentially the same as that described in reference 3. The major difference in the set-up is that for the present tests an air-cooled radial engine furnished the motive power. This engine required a nacelle larger than that used in the earlier tests and of somewhat different shape. A photograph of the set-up is shown in figure 1, and a schematic diagram in figure 2.

Engine and nacelle.- In this series of tests the propeller was driven by a Pratt and Whitney R-1340 radial air-cooled engine. The power rating of this engine is 550 horsepower at 2100 rpm. The propeller was driven directly at crank shaft speed, and was turned up to 2300 rpm at the low-blade-angle settings. The rotational speed of the engine and propeller was measured with a condenser tachometer which was not in error by more than ±1/2 percent, above 1000 rpm.

The engine cowling-nacelle combination was arranged to give as good cooling as was compatible with relatively low impedance to the propeller slipstream.

Propellers.- Three sets of Curtiss propeller blades differing only in blade section were investigated. The blades designated by drawing number 89306-22S embodied Clark Y sections and were tested both as two bladed and three bladed propellers. Propeller number 101336 was made with doubld cambered Clark Y sections and was tested only as a two bladed propeller. Propeller number 101332 was made with Clark Y sections inboard from the 0.50R station, and with NACA 16-series from the 0.70R station to the tip. At stations between 0.50R and 0.70R transition sections from Clark Y to 16-series sections were used. The NACA 16-series sections, described in reference 4, have relatively sharp leading and trailing edges, and have maximum thickness at the mid-chord station. They are designed to work efficiently at high speed by delaying the compressibility stall. Propeller number 101332 was designed originally with seriously modified 16-series sections. The modification was a large increase in the leading edge and trailing edge radii and a corresponding thickening of the leading and trailing edges. In this report the Curtiss design 16-series sections are designated as the "modified 16-series" sections. Blades with these sections were tested as a two bladed propeller. After being tested these blades were returned to the factory and the sections from 0.70R to the tip altered to conform more nearly to the true NACA 16-series shape and are designated herein as the reworked 16-series section. These reworked blades were tested both as two bladed and three bladed propellers. Blade form curves for the three propellers are shown in figure 3. Blade sections at the 0.70R are shown in figure 4. The section at the 0.70R rather than that at the 0.75R was chosen because of the significance of the 0.70R station in Driggs' method of propeller analysis.

TESTS

Each test was made at one blade angle setting. Beginning at about 600 rpm, the net thrust, torque, and propeller rotational speed were measured simultaneously at various intervals until the highest speed obtainable under 2300 rpm was reached. Readings were taken at speed intervals of about 100 rpm at low speeds, and at much smaller intervals near the top speed. Each propeller was tested at a series of blade angles from 0° to 20° by intervals of approximately 2°. The blade angle was measured at three-quarters radius. Before and after each run the wind velocity was measured with an anemometer. Tests were made only when the wind velocity was less than five miles per hour, except in one or two tests at high blade angles.

RESULTS

The results of the static propeller tests are presented in terms of conventional coefficients:

$$C_T = \frac{T_e}{\rho\ n^2\ D^4}, \text{ thrust coefficient}$$

$$C_P = \frac{P}{\rho\ n^3\ D^5}, \text{ power coefficient}$$

$T_e = T - \Delta D$, effective thrust, pounds

T, tention in propeller shaft, pounds

ΔD, the force exerted by the propeller slipstream on the nacelle and struts, pounds

P, $2\pi n Q$, engine power, foot-pounds per second

Q, engine torque, pound - feet

ρ, mass density of air, slugs per cubic foot

n, propeller rotational speed, revolutions per second

$D = 2R$, propeller diameter, feet

R, propeller tip radius, feet

$\frac{C_T}{C_P}$ = static thrust figure of merit

$M = \frac{\pi n D}{c}$, tip speed ratio

c = speed of sound in air, feet per second

$J = V/nD$, advance ratio

V, air speed, feet per second

$\eta = \frac{C_T}{C_P} J$, propeller efficiency

$q = 1/2 \rho V^2$, dynamic pressure, pounds per square foot

L, lift, pounds

D, profile drag, pounds

S, area, square feet

$C_L = \frac{L}{q S}$, lift coefficient

$C_D = \frac{D}{q S}$, profile drag coefficient

Table I

Description of the figures.

1. Photograph, static propeller test rig.

2. Diagram of static thrust and torque set-up.

3. Blade form curves.

4. Propeller blade sections at the 0.70R.

5 - 16. Variation of static thrust and power coefficients with tip-speed ratio and blade angle.

17 - 28. Static propeller characteristics as functions of blade angle.

29 - 33. Comparisons of static thrust figure of merit.

34 - 39. Lift and drag coefficients computed from static propeller characteristics.

40. Envelope efficiencies computed by Driggs' method from static propeller data.

DISCUSSION

In this series of static propeller tests, made for comparing the Clark Y airfoil propeller section with the modified and reworked 16-series sections, the independent variables used were blade angle and propeller rotational speed. Blade angle was fixed for each test, hence changes in propeller characteristics during a run must be attributable only to changing propeller rotational speed. At least three factors which affect the behavior of the propeller blade sections are functions of the rotational speed. Of first importance is the increase with tip-speed ratio of the Mach number at which the blade sections work, and the changes in blade section airfoil characteristics with Mach number. A secondary effect of increase in rotational speed is an increase in the Reynold's number at which the blade sections work. A third factor, of unknown influence, is the tendency of the propeller blade to discard by centrifugal force the retarded air composing the boundary layer. Both of the latter two factors have a beneficial influence on the performance of the blade sections. Even at a tip speed much below that for normal operation most of the propeller sections work at values of the Reynold's number greater than the critical; hence as the Reynold's number is increased blade section profile drag coefficient is reduced and maximum lift coefficient is increased. Centrifugal force may act to remove a part of the air in the boundary layer; this would delay the normal stall.

Apparently the only adverse effect accompanying high propeller tip speed is due to the behavior of airfoils in compressible flow as the air speed approaches the acoustic velocity. Wind-tunnel tests, reference 5, have shown that both the lift and drag coefficients of an airfoil increase with increasing Mach number until a critical value is reached. This value is believed to be reached when the local air velocity at some point on the airfoil is equal to the acoustic velocity. As the Mach number is increased beyond the critical value the lift coefficient decreases while the drag coefficient increases more rapidly than it does at subcritical values of the Mach number. Only the net influence of the several factors is measured by static propeller tests. Therefore, the adverse effect of air compressibility on blade section behavior at high tip speed, being partially offset by beneficial factors, is not as fully discernible from static propeller tests as from wind-tunnel tests on airfoils.

While the tests were being made it was noticed during each run that the character of the noise emitted by the engine and propeller began to change from a roar to a penetrating note at about 1800 rpm. The propeller diameter was ten feet. This may indicate that the first shock waves are set up at the propeller tips at a tip speed ratio of about $M = 0.82$. The region of the propeller blade tip producing a shock wave spreads inwardly as the tip speed ratio increases. Since the highest value of the tip speed ratio obtained in these tests was M = 1.05, only those sections at radii greater than 0.78R were working at a value of Mach number greater than 0.82. The effect of compressibility indicated in the figures was produced in most cases by a relatively small outer portion of the propeller blades.

The basic pitch distribution for the propeller blades subject to these tests was about 20° at the three-quarters radius. This pitch distribution will give highest propeller efficiencies within a range of advance ratio between J = 0.75 and J = 1.50. A high basic pitch distribution results in a tendency for a propeller in static tests to yield less thrust for a given power than a similar propeller with less blade twist. It is this fact which discredits the propeller polars and efficiency curves computed by the single point method from the results of static tests and confines their usefulness to qualitative comparisons.

The data presented in the figures have been corrected for any small mean wind velocity that held during the tests. The variation of static thrust coefficients with tip speed ratio shown in figures 5, 7, 9, 11, 13, and 15 agrees with the results of wind-tunnel tests on airfoils. The increasing static thrust coefficient with increasing tip speed ratio indicates that, when blade sections near the tip are working at positive lift, the lift coefficients increase with increasing Mach number up to a certain point. The lower rate of increase of the static thrust coefficient as tip-speed ratios approach unity indicates a decrease of the lift coefficients of sections near the blade tip as the Mach number at which they operate approaches unity. The increasing static thrust coefficients with increasing tip-speed ratio produced at high blade angles even at low values of the tip-speed ratio may be partially attributable to Reynold's number effect and to the beneficial action of centrifugal force in throwing off dead air from the stalled region of the propeller.

The variation of static power coefficient with tip-speed ratio shown in figures 6, 8, 10, 12, 14, and 16, also agrees with wind-tunnel tests on airfoils. The slight decrease of the static power coefficients with increasing tip speed ratio at low values of the tip-speed ratio may be due to decreasing drag coefficients of the blade sections with increasing Reynold's number. For the blade settings which yield positive lift near the tip the gradually increasing power coefficients at tip-speed ratios of about M = 0.7 or M = 0.8 again indicate the increase of lift and drag coefficients of airfoils working at Mach numbers below the critical. The sharper rise of the power coefficients, for all blade settings, as the tip-speed ratio approaches unity is comparable to the rapid increase of airfoil drag coefficients as the Mach number approaches unity.

Figures 17 through 28 are cross plots of figures 5 to 16, inclusive, at tip-speed ratios of M = 0.9 and M = 1.0. The static thrust and power coefficients and static thrust figure of merit are shown as functions of blade angle at the three-quarters radius. The similarity of this manner of presenting propeller data to airfoil lift and drag coefficients as functions of angle of attack is pointed out in reference 3.

The relative merits of propeller sections may be shown best by the comparison of properties independent of blade angle. Figures 29 through 33 present comparisons of the static thrust figures of merit plotted against power coefficient at values of tip-speed ratio of M = 0.5, 0.7, 0.9, 1.0, and 1.1. A study of these figures leads to the following generalizations:

(1) There is little difference between the behavior of the reworked 16-series sections and that of the modified 16-series sections.

(2) The double-cambered Clark Y section gives results very similar to those for the reworked 16-series sections, though slightly inferior.

(3) At low tip-speed ratios and under high loading the single-cambered Clark Y section is superior to all other sections used in these tests.

(4) At high tip-speed ratios both the modified and reworked 16-series sections are superior to the Clark Y sections.

(5) Under small load a two-bladed propeller gives more thrust per horsepower than a three-bladed propeller, but under high loading the reverse is true.

In actual flight the propeller tip-speed ratios encountered most frequently are close to $M = 0.9$, and at that tip-speed ratio the data presented here are most reliable. The static thrust figures of merit in figure 31 for $M = 0.9$ show that over a small range the reworked 16-series section is superior to the other sections; the modified 16-series section is good over a broader range of power coefficient, the double-cambered Clark Y is only slightly inferior to the modified 16-series section; and the single-cambered Clark Y shows up to advantage only at the high values of the power coefficient. In figure 32, at a tip-speed ratio of $M = 1.0$, both the modified and reworked 16-series sections show worthwhile superiority over the Clark Y sections over the range of power coefficients obtainable in these tests. In the range of tip-speed ratios from $M = 0.9$ to $M = 1.0$, which is realized in practice at high altitude, the mean superiority of the 16-series section over the single-cambered Clark Y propeller section appears to be about three percent. The computed propeller lift coefficients corresponding to the range of 16-series superiority lie between $C_L = 0.3$ and $C_L = 0.6$. At higher lift coefficients obtained during take-off and climb the Clark Y propeller section is superior except at very high tip-speed ratios.

The trend of the curves in figures 31, 32, and 33 indicates that at very high values of the power coefficient the Clark Y propeller may be superior to the 16-series propeller even at high values of the tip-speed ratio.

Such low power was available for the present tests that high tip-speeds could not be attained at high blade angles and the effect of blade stalling does not show up at high tip-speed ratios as markedly as at the low tip-speed ratios and higher blade angles. In a report by the Curtiss Company of flight and Wright Field static tests of the subject propellers, reference 6, the results of tests using higher power coefficients are reported. The following values are taken from this reference.

Blade section	Clark Y	Clark Y and 16-series
Thrust/horsepower	3.08	2.78
Percent	100.0	90.0

The foregoing values were obtained with a three-bladed propeller when $C_P = 0.103$ and $M = 0.84$ in standard air, and correspond to the following values of static thrust figure of merit and computed propeller lift coefficient:

Blade section	Clark Y	Clark Y and 16-series
C_T/C_P	1.68	1.52
C_L	1.23	1.11

The above comparison indicates the superiority of the Clark Y propeller over the 16-series propeller when operating at high values of the lift coefficient encountered at take-off and during climb. This is in agreement with the results of wind-tunnel tests reported in reference 1.

A similar comparison of three-bladed propellers having Clark Y and 16-series sections is presented in table II. The peak values of the thrust figure of merit and the corresponding values of power coefficient were taken from figures 29 through 33.

Table II

	CLARK Y				CLARK Y AND 16-SERIES			
M	C_P	C_T/C_P	C_L	Percent	C_P	C_T/C_P	C_L	Percent
0.5	0.020	2.75	0.36	97	0.017	2.85	0.32	100
0.7	0.018	3.00	0.35	100	0.015	3.01	0.30	100
0.9	0.017	2.95	0.33	97	0.018	3.03	0.36	100
1.0	0.020	2.61	0.34	92	0.020	2.83	0.37	100
1.1	0.030	1.95	0.38	84	0.029	2.32	0.44	100

This latter comparison shows that a propeller embodying 16-series sections will yield about three percent more thrust than a Clark Y propeller of similar form when operating conditions are such that the blade sections work at lift coefficients between $C_L = 0.30$ and $C_L = 0.40$.

The results in table II are encouraging in that they indicate the design possibilities of the NACA 16-series sections.

The tip sections of propeller No. 101332, identical with those for propeller No. 101330, were the reworked 16-series sections designed to operate best at lift coefficients between $C_L = 0.30$ and $C_L = 0.40$. These design lift coefficients are given in reference 7, and are plotted in figure 3. The propeller lift coefficients for the reworked 16-series propeller computed from these static tests at peak values of static thrust figure of merit are bracketed between $C_L = 0.30$ and $C_L = 0.44$, and are practically identical with the design lift coefficients. In this range of lift coefficient values the reworked 16-series sections are superior to all other sections used in these tests. Inasmuch as the NACA 16-series sections can be designed for best operation at any reasonable value of the lift coefficient, reference 4, it is reasonable to believe that a propeller can be made embodying the NACA 16-series sections which will be superior to any similar propeller embodying Clark Y sections, when operating conditions are such that the design lift coefficients are realized. The range of lift coefficient values for superior performance of the NACA 16-series sections extends appreciably in both directions from the design value. It is possible that propeller No. 101332 would have shown up much better for take-off and climb with little sacrifice of efficiency at high speed if the tip sections had been designed for optimum operation at higher values of the lift coefficient. Further improvement in take-off and climbing characteristics may be had by taking advantage of the good high speed operation of 16-series sections and using higher tip speeds, and by increasing the blade area.

Propeller efficiency is equal to the product of thrust figure of merit multiplied by advance ratio, ($\eta = C_T/C_P \times J$). The value of the thrust figure of merit necessarily decreases as the advance ratio increases. If the relative values of the thrust figures of merit of the sections do not change with advance ratio, about three percent greater maximum efficiency may be expected of a propeller embodying the reworked 16-series sections than from one made with the single cambered Clark Y sections, when the tip-speed ratio is close to M = 0.9 or M = 1.0.

In static tests the axial velocity through the propeller is relatively small. When a propeller is in actual operation advancing at a normal high speed, the blade section resultant velocity of rotation and advance is considerably higher than the velocity due to rotation alone and consequently the region of the propeller tip suffering a compressional loss extends considerably farther inboard. The propeller losses at high tip-speed ratios indicated by static tests will most likely be exceeded in flight.

The lift and profile drag coefficients computed by the method given in reference 2 from static propeller characteristics are presented as polars in figures 34 through 39. These of necessity yield the same information as the static thrust figure of merit comparisons, though in a more familiar form. This method of propeller blade section analysis regards the propeller as an airfoil acting at the seven-tenths radius station. For all blade sections the value of the minimum drag coefficient does not change much in the interval of tip-speed ratios from $M = 0.5$ to $M = 0.9$. The drag coefficients increase rapidly with increasing tip-speed ratio when the value of the latter exceeds $M = 0.9$.

The polars in figures 34 to 39, inclusive, do not represent absolute values of the airfoil characteristics, but are for comparison only. The unusually large values of the drag coefficients shown by these polars may be due both to the propeller pitch distribution and to impedance to the propeller slipstream by the cowling and nacelle.

The polars for the three-bladed propellers shown in figures 35 and 39 have been used in applying Driggs' method for computing propeller efficiency envelopes. Since the polars show only relative values, the computed efficiency curves likewise can show only relative values. The absolute values near maximum efficiency are about eight percent lower than those obtained in wind-tunnel tests on the same propellers with a well streamlined body, reference 1. Figure 40 shows a comparison of the computed envelope efficiency curves of two three-bladed propellers, numbers 101332 and 89306-22S, identical in all respects except blade section. The assumed power available is that which may be obtained from a 1100 horsepower engine. The 10 foot 4 inch diameter propeller is assumed to operate at 1500 rpm. In these computations the actual propeller tip-speed ratio was used rather than rotational tip-speed ratio.

Figure 40 presents relative efficiencies at sea level. Due to the low maximum lift coefficients obtainable with the reworked 16-series tip sections the Clark Y propeller is superior at the low values of advance ratio encountered during take-off and climb. At high values of the advance ratio where the blade sections work at lower lift coefficients and where the effect of compressibility becomes noticeable the propeller having 16-series sections is more efficient. The two propellers are apparently of equal efficiency at sea level at a value of the advance ratio of about $J = 1.7$. At practical values of the advance ratio above $J = 1.7$ the 16-series propeller may yield as much as two percent higher efficiency than the Clark Y propeller at sea level, and as much as three percent higher at 15,000 feet altitude where greater tip-speed ratios obtain.

REMARKS

1. For all of the propellers tested the highest value of the static thrust figure of merit occurred at a tip-speed

ratio between $M = 0.7$ and $M = 0.9$; hence in flight highest efficiency may be expected in the same range of tip-speed ratios.

2. There is little choice between the reworked 16-series sections and the modified 16-series section with rounded leading and trailing edges. Both are superior to the Clark Y sections in the region of peak value of the thrust figure of merit, i.e., under small load.

3. The double-cambered Clark Y section is similar in behavior to the 16-series sections; the efficiency is lower at the peak static thrust figure of merit but higher at relatively high values of the power coefficient.

4. The propellers having modified and reworked 16-series blade sections were found to stall at lower values of the lift coefficient than did the propeller with single-cambered Clark Y sections, at low values of the tip-speed ratio. This agrees with wind-tunnel tests which indicate the superiority of the Clark Y propeller for take-off and climb. On the basis of these static tests the superiority of the Clark Y propeller for take-off and climb holds for values of tip-speed ratio less than $M = 0.9$.

5. Envelope propeller efficiencies computed from these static data indicate that a Clark Y propeller of the design tested yields appreciably higher efficiency during take-off and climb than a similar propeller with reworked 16-series

sections. The 16-series propeller shows one or two percent higher efficiency than the Clark Y propeller at high speeds attainable with airplanes now existent, and a possible greater gain when used with higher speed airplanes.

6. It is to be understood that the conclusions reached from these tests with regard to the 16-series sections applies only to sections designed to operate most effectively at lift coefficients between $C_L = 0.30$ and $C_L = 0.40$.

7. It is probable that better take-off and climb operation could be obtained from a 16-series propeller designed to operate best at higher values of the lift coefficient than those for which the subject propeller was designed.

8. Redesign of the 16-series propeller with greater blade area and for higher tip speeds might produce a propeller with much better take-off characteristics with little sacrifice of efficiency at high speed.

Langley Memorial Aeronautical Laboratory,
National Advisory Committee for Aeronautics,
Langley Field, Va., August 27, 1941.

REFERENCES

1. Gray, W. H.: Wind-Tunnel Tests of Four Curtiss Propellers Embodying Different Blade Sections. NACA MR, Aug. 21, 1941.

2. Driggs, Ivan H.: Simplified Propeller Calculations, Jour. Aero. Sci., vol. 5, no. 9, July 1938, pp. 337-344.

3. Hartman, Edwin P., and Biermann David: Static Thrust and Power Characteristics of Six Full-Scale Propellers. NACA Rep. No. 684, 1940.

4. Stack, John: Tests of Airfoils Designed to Delay the Compressibility Burble. NACA TN No. 976, Dec. 1944. (Reprint of ACR, June 1939.)

5. Stack, John, Lindsey, W. F., and Littell, Robert E.: The Compressibility Burble and the Effect of Compressibility on Pressures and Forces Acting on an Airfoil. NACA Rep. No. 646, 1938.

6. Anon.: Comparison of Flight Test on Propellers Using Clark-Y, N.A.C.A.-16 and Combination Clark-Y and N.A.C.A.-16 Profiles. Rep. No. C-1123, Curtiss Propeller Div., Curtiss-Wright Corp., Nov. 11, 1940.

7. Anon.: Aerodynamic Analysis of Curtiss Propeller Blade Designs 89306-22S and 101330 as Applied to the Normal V_{max} Flight Condition of the Curtiss Hawk 75A. Rep. No. C-1083, Curtiss Propeller Div., Curtiss-Wright Corp., June 3, 1940.

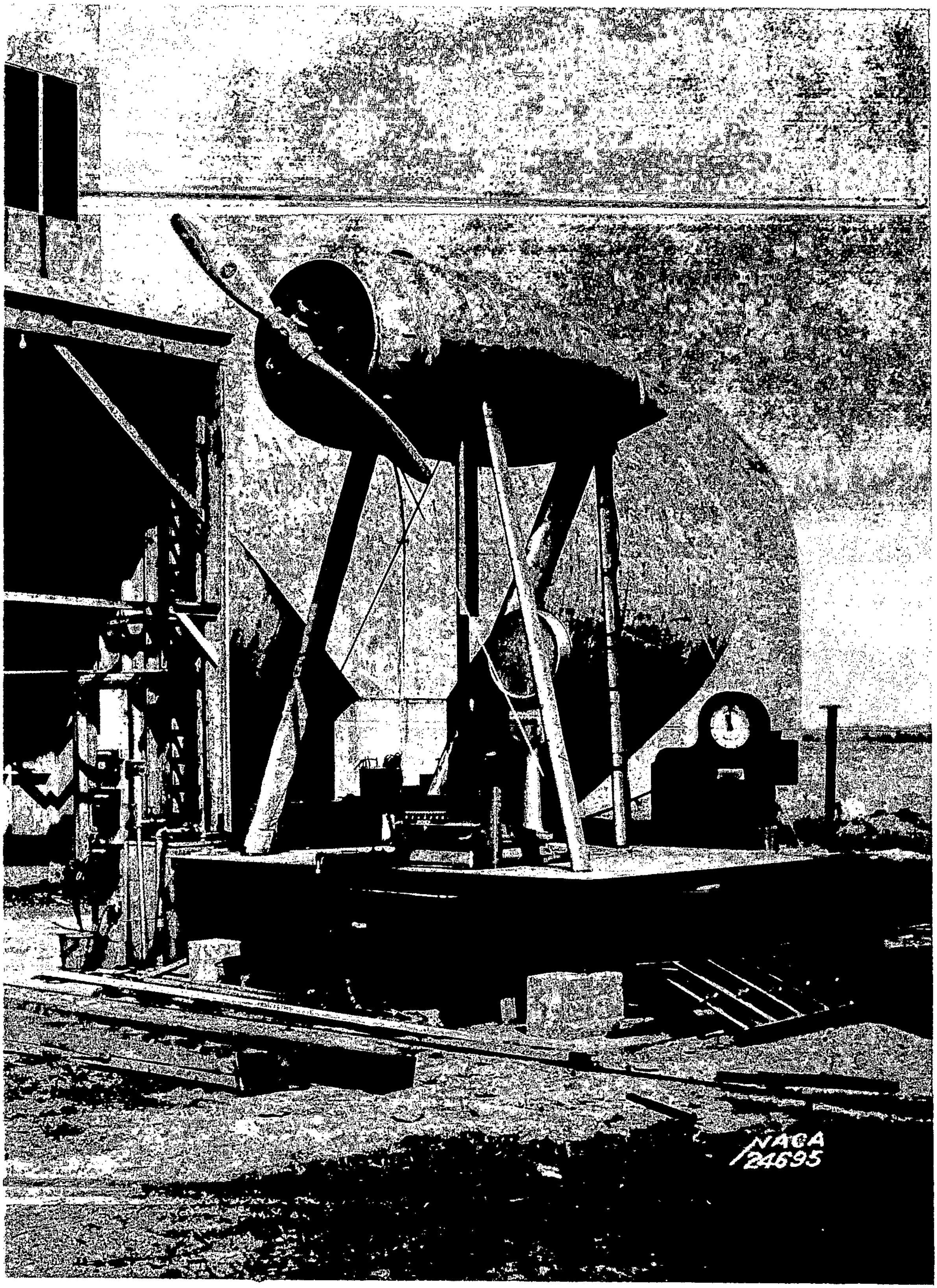

Figure 1.- Static propeller test rig.

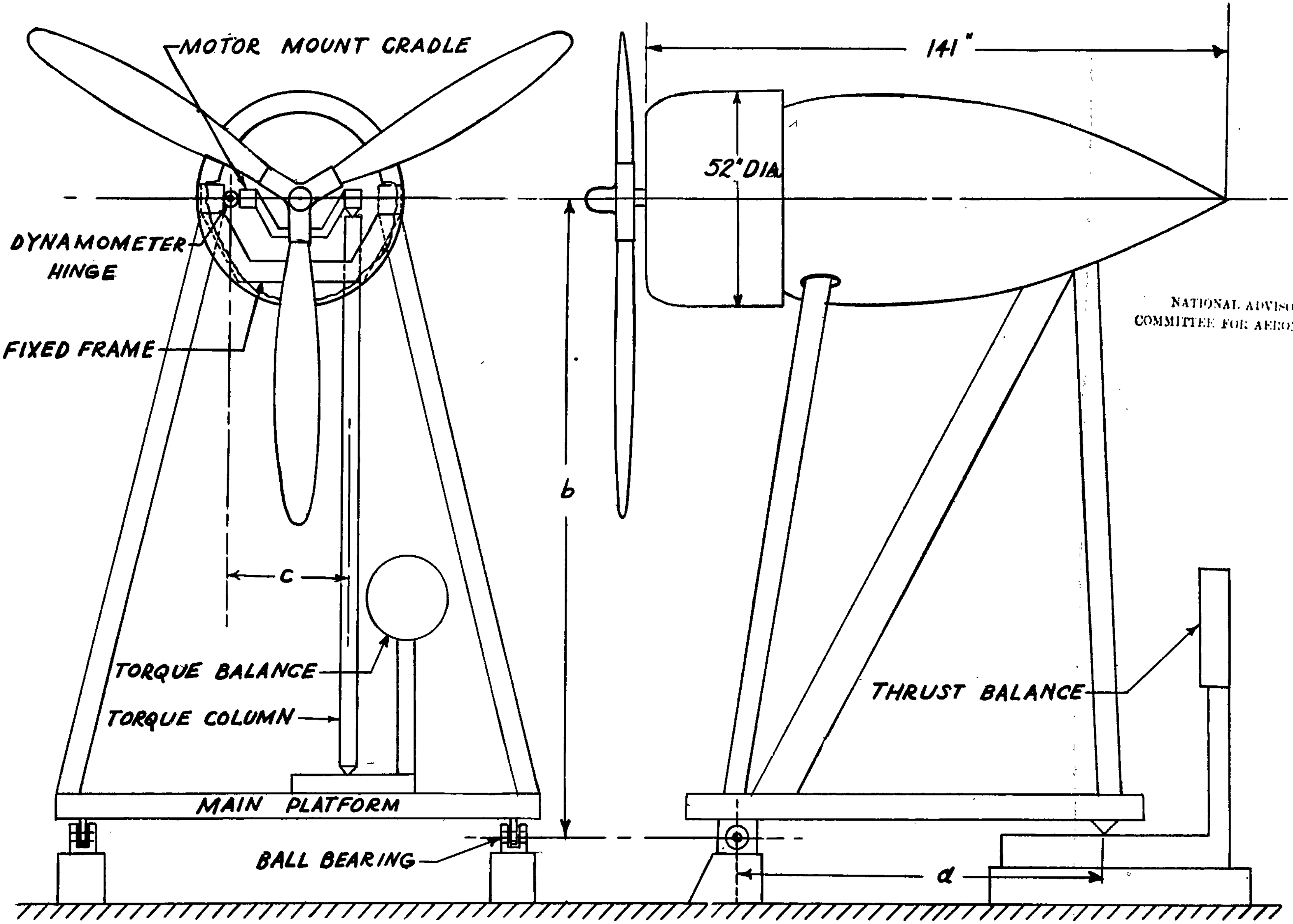

Figure 2.- Diagram of static thrust and torqué set-up.

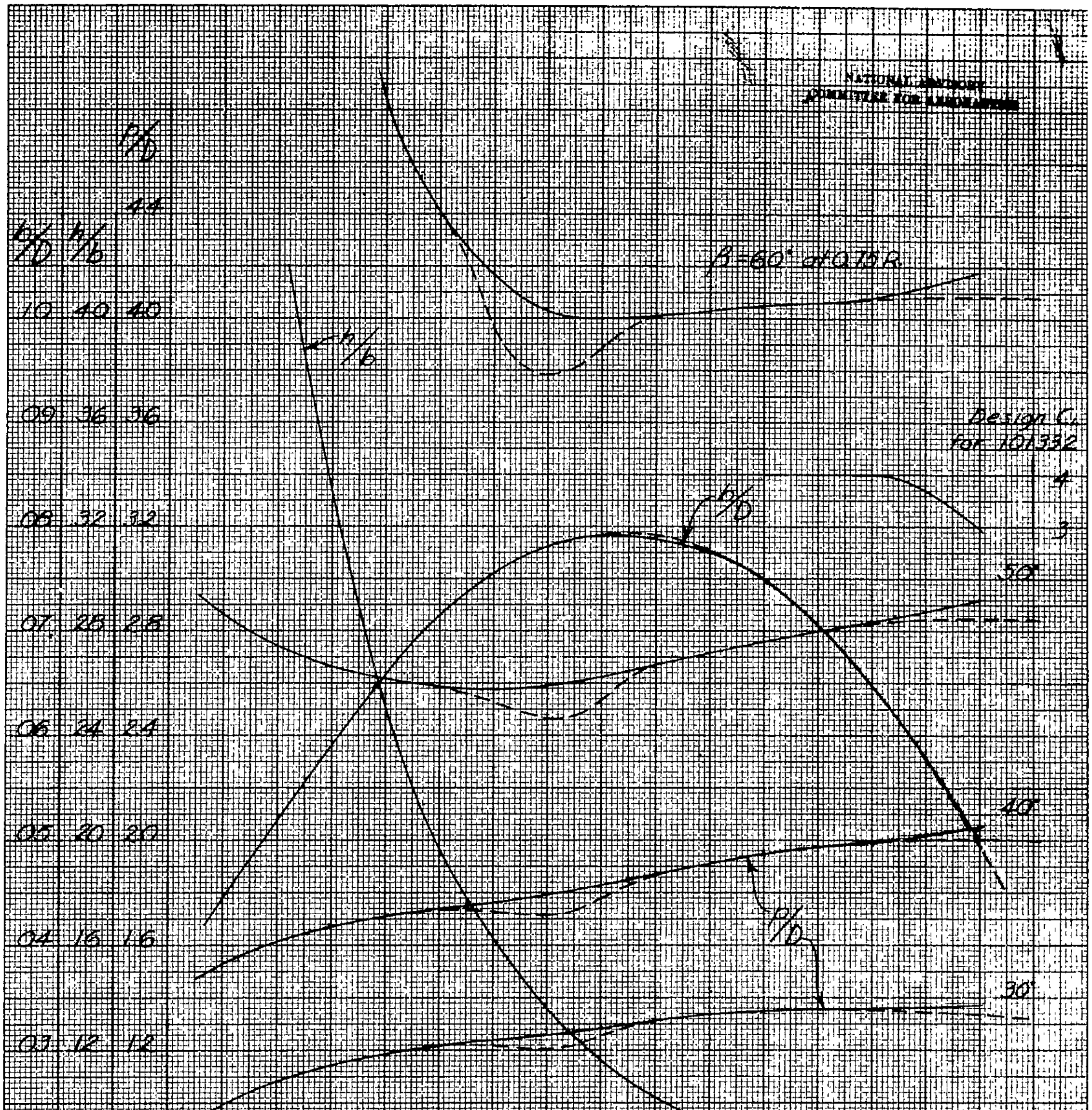

Figure 3.-Plan-form curves for three Curtiss propellers.
D, diameter; R, radius to tip; r, station radius;
b, section chord; h, section thickness; p, geometric
pitch; β, blade angle.

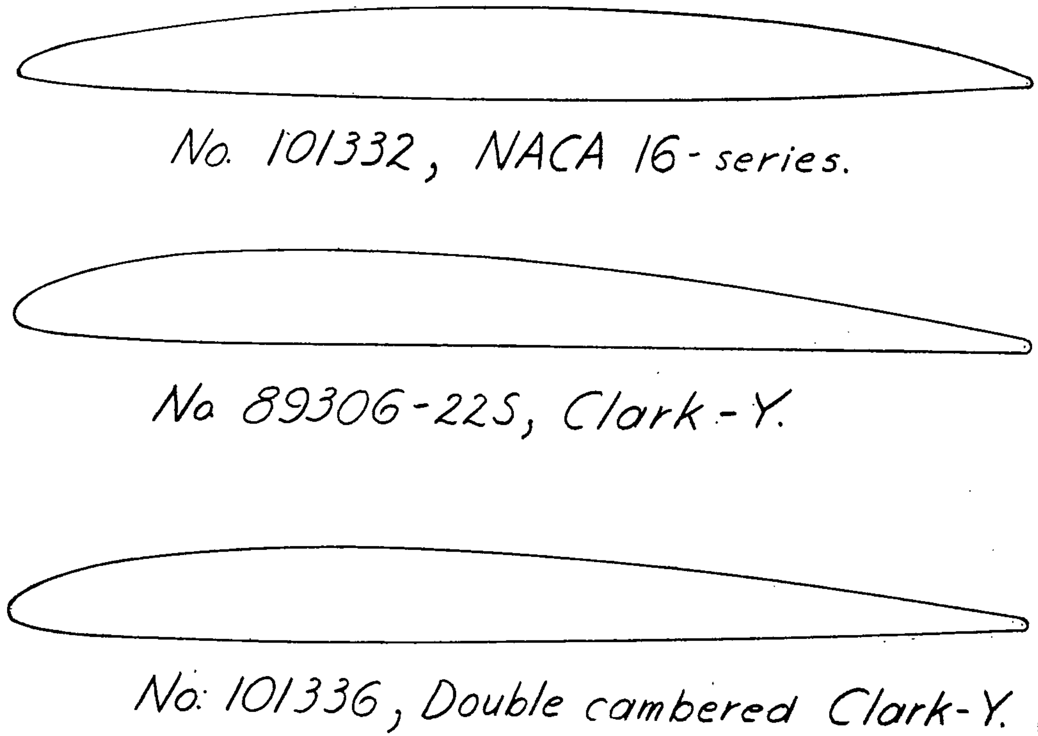

Figure 4. - Propeller blade sections at the 0.70R.

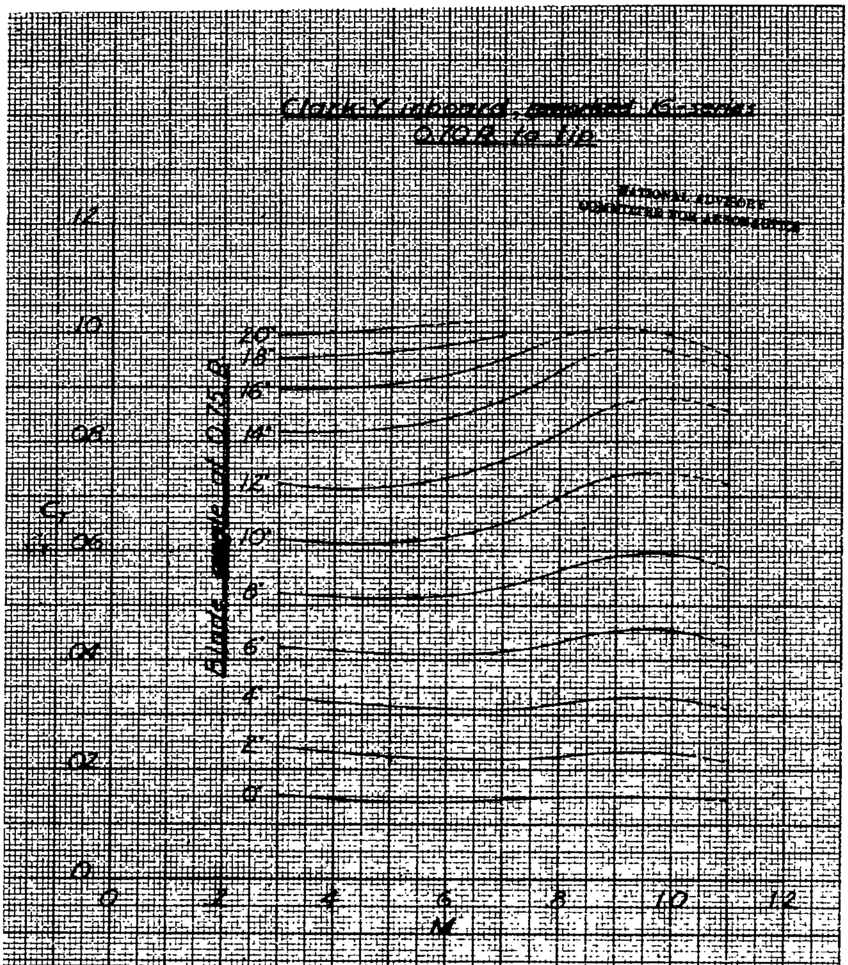

Figure 5. Variation of static thrust coefficient with tip-speed ratio and blade angle. Two bladed propeller No. 101332

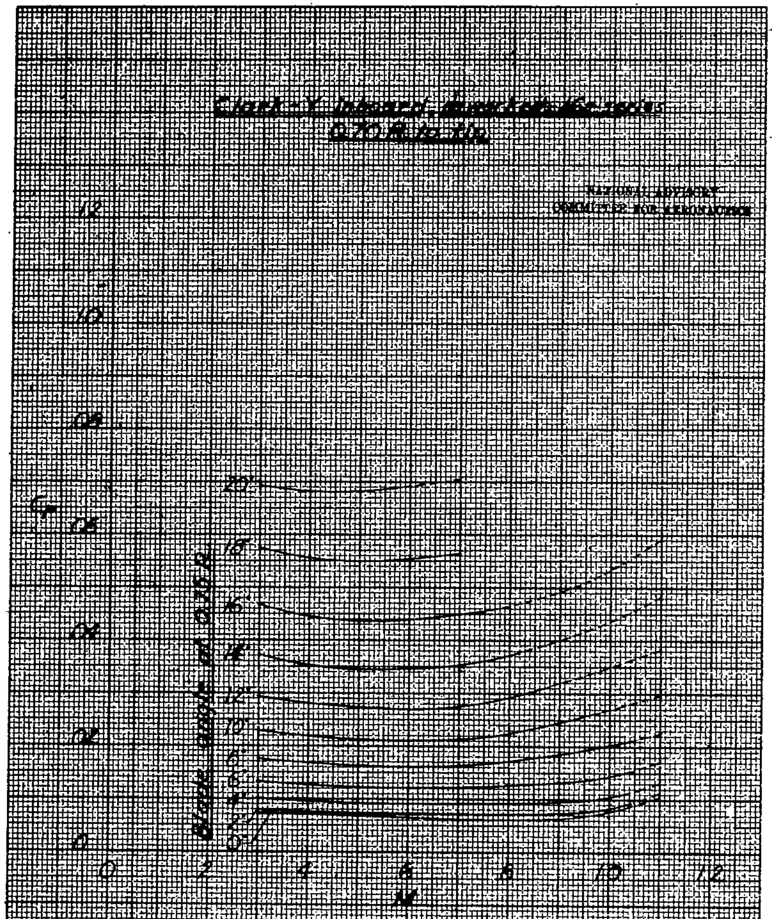

Figure 6. - Variation of static power coefficient with tip-speed ratio and blade angle. Two-bladed propeller No. 1015R.

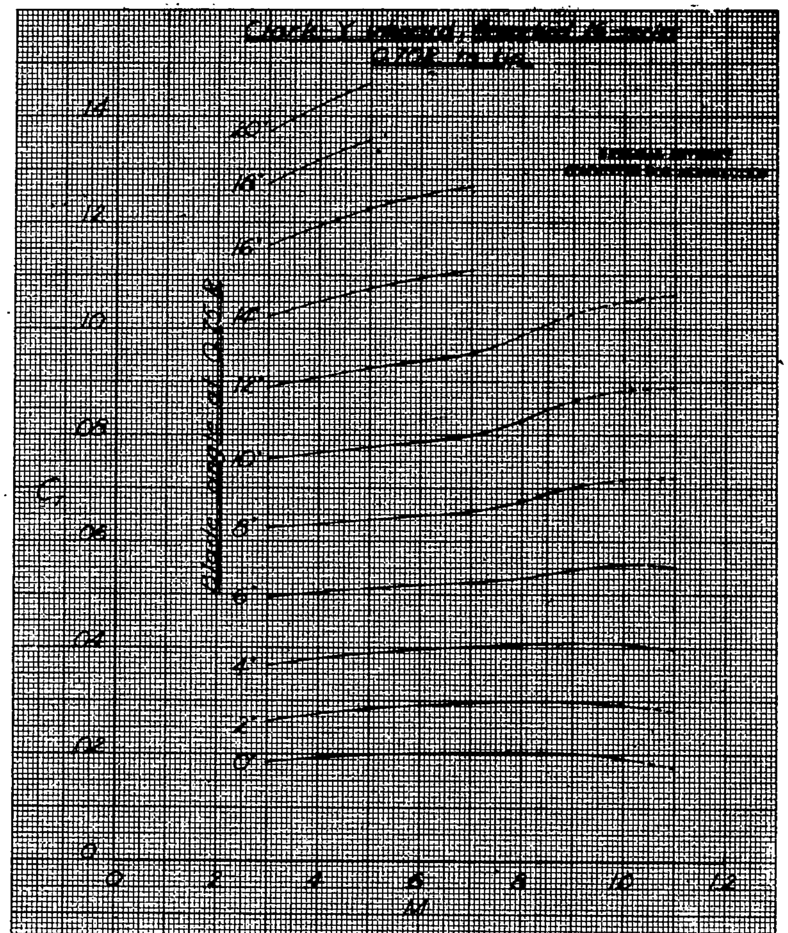

Figure 7. - Variation of static thrust coefficient with tip speed ratio and blade angle. Three bladed propeller No. 10432.

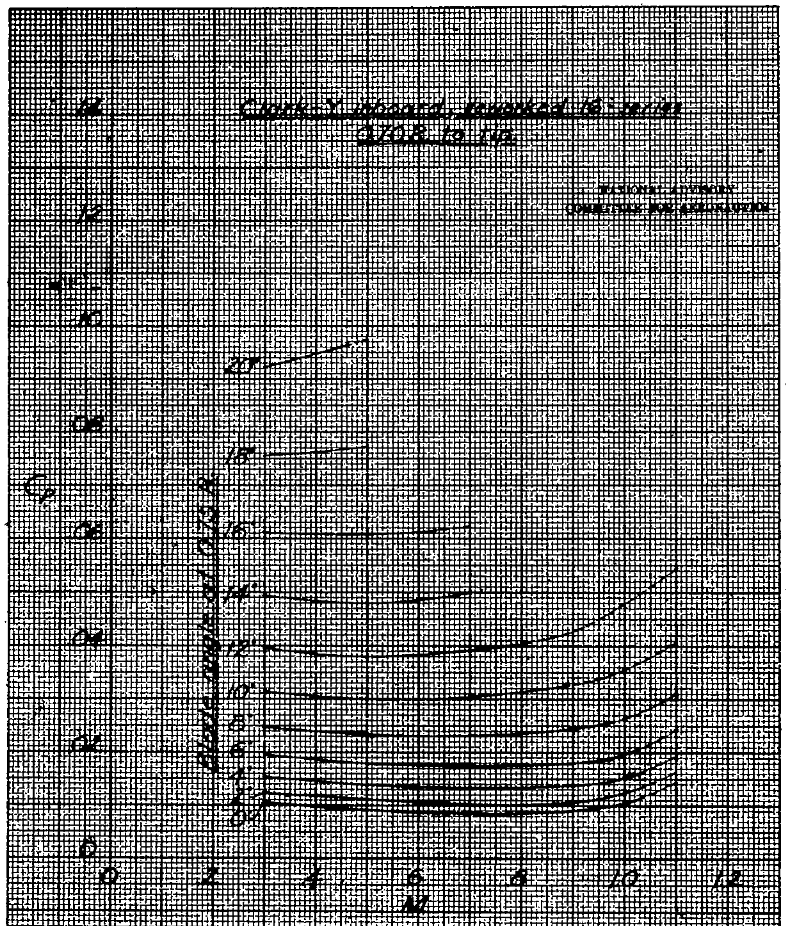

Figure 8. - Variation of static power coefficient with tip-speed ratio and blade angle. Three bladed propeller No. 101332.

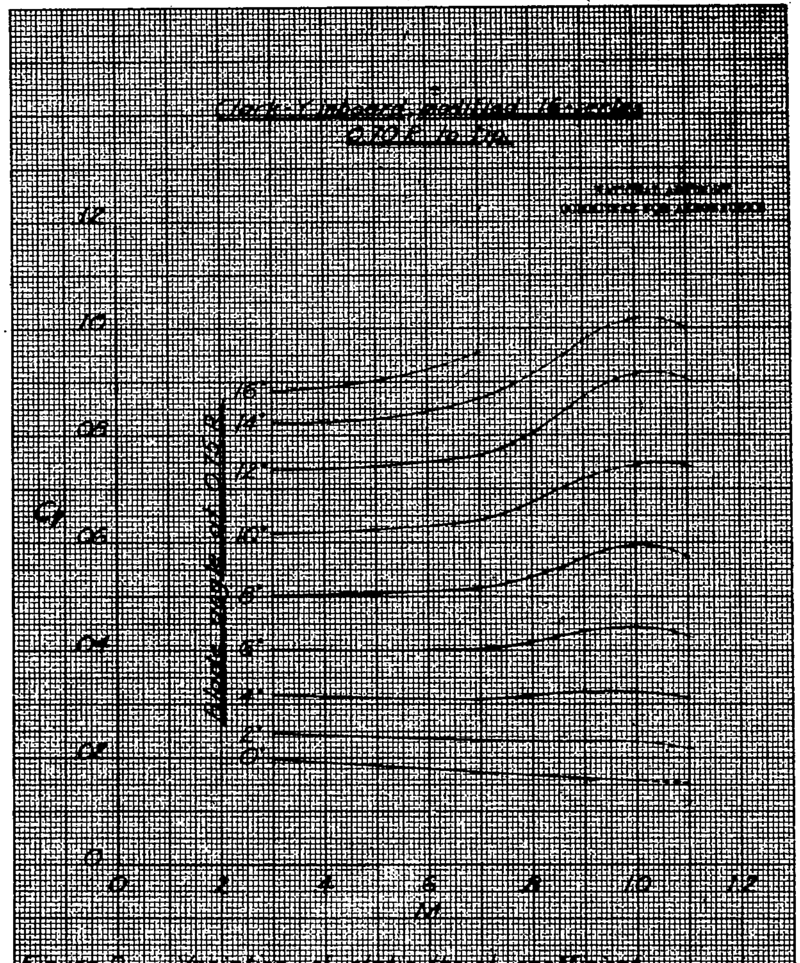

Figure 9. Variation of static thrust coefficient with tip-speed ratio and blade angle. Two bladed propeller No. 101332.

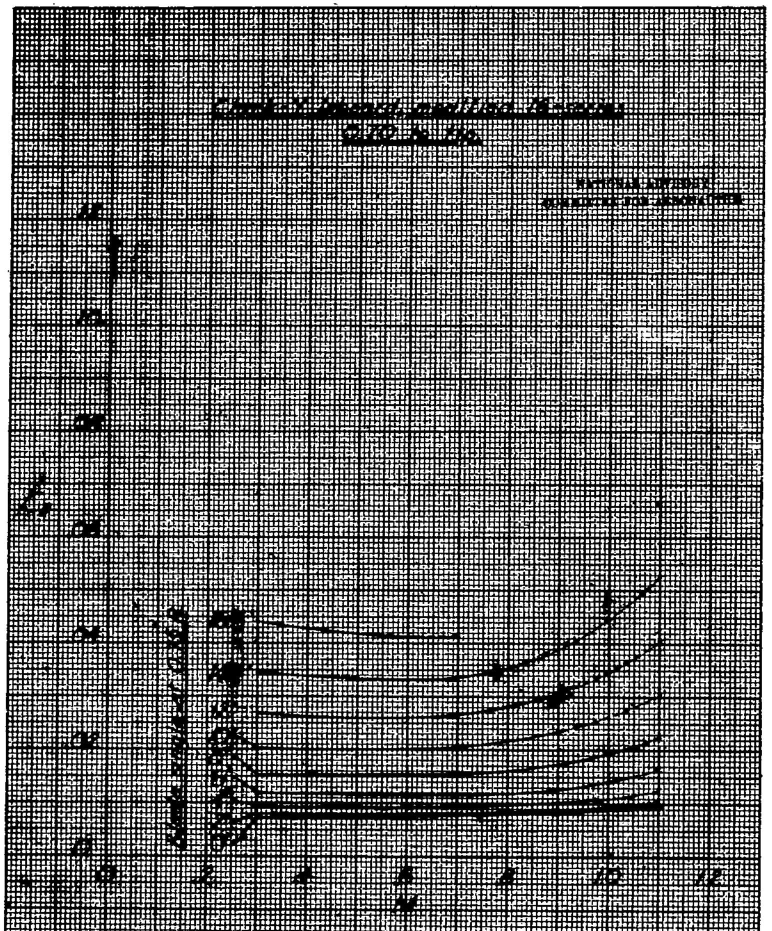

Figure 10.- Variation of static power coefficient with tip-speed ratio and blade angle. Two-bladed propeller No. 101332.

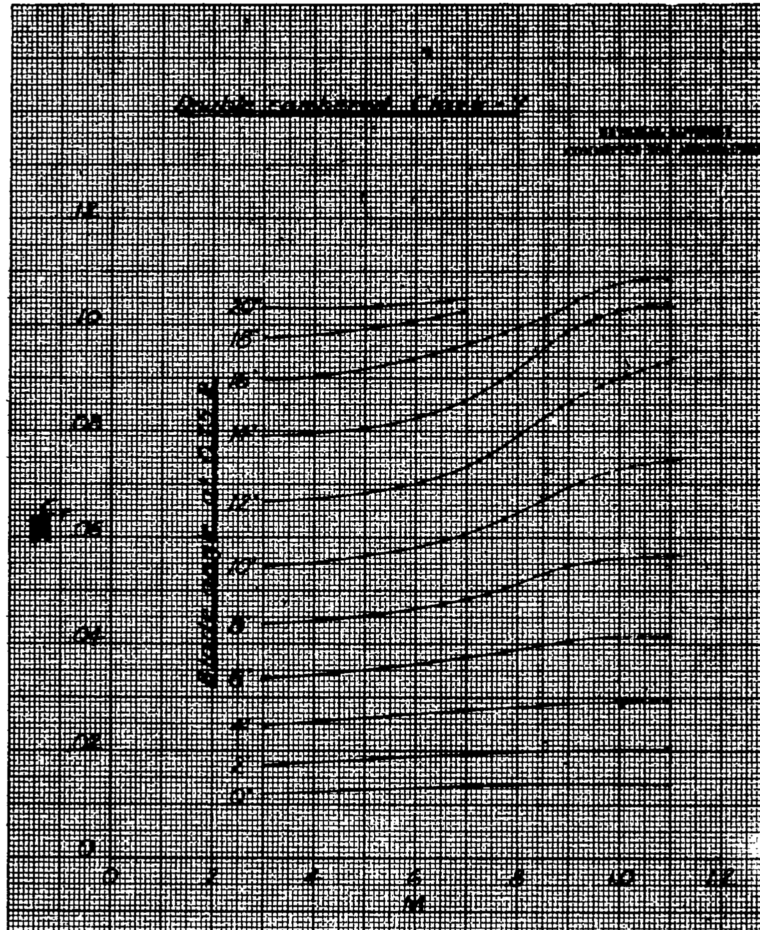

Figure 11.- Variation of static thrust coefficient with tip-speed ratio and blade angle. Two-bladed propeller No. 101336.

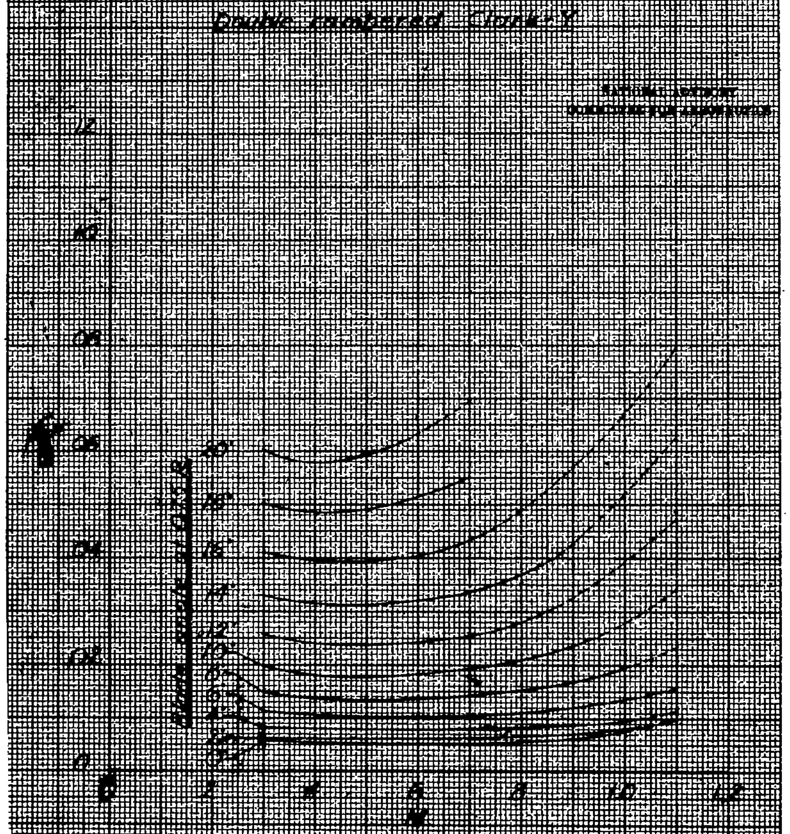

Figure 14. - Variation of static power coefficient with tip-speed ratio and blade angle. Two bladed propeller No. 101356.

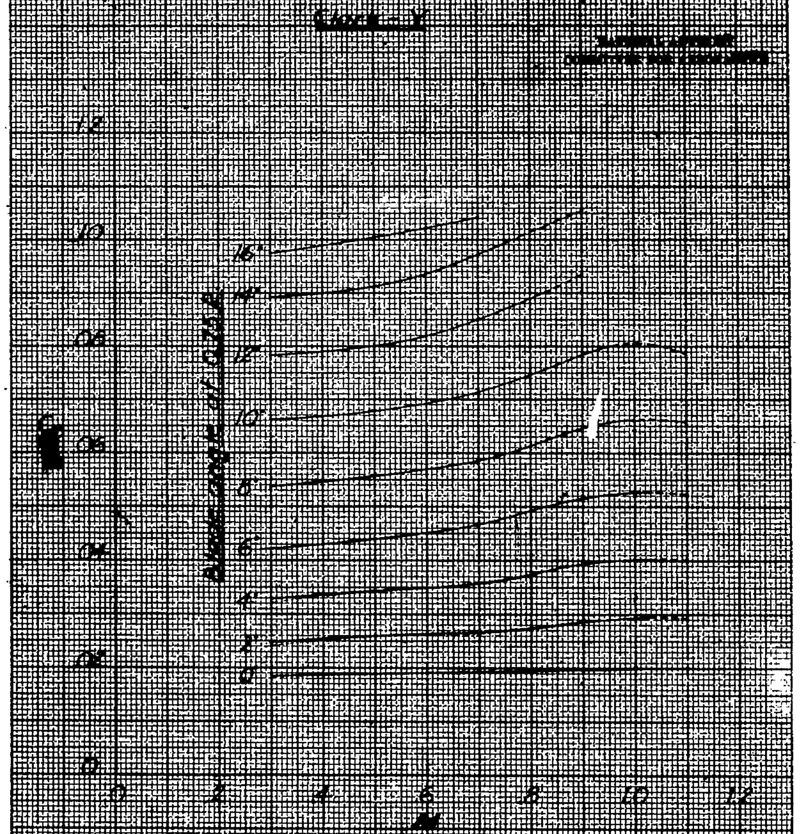

Figure 15. - Variation of static thrust coefficient with tip-speed ratio and blade angle. Two bladed propeller No. [illegible]

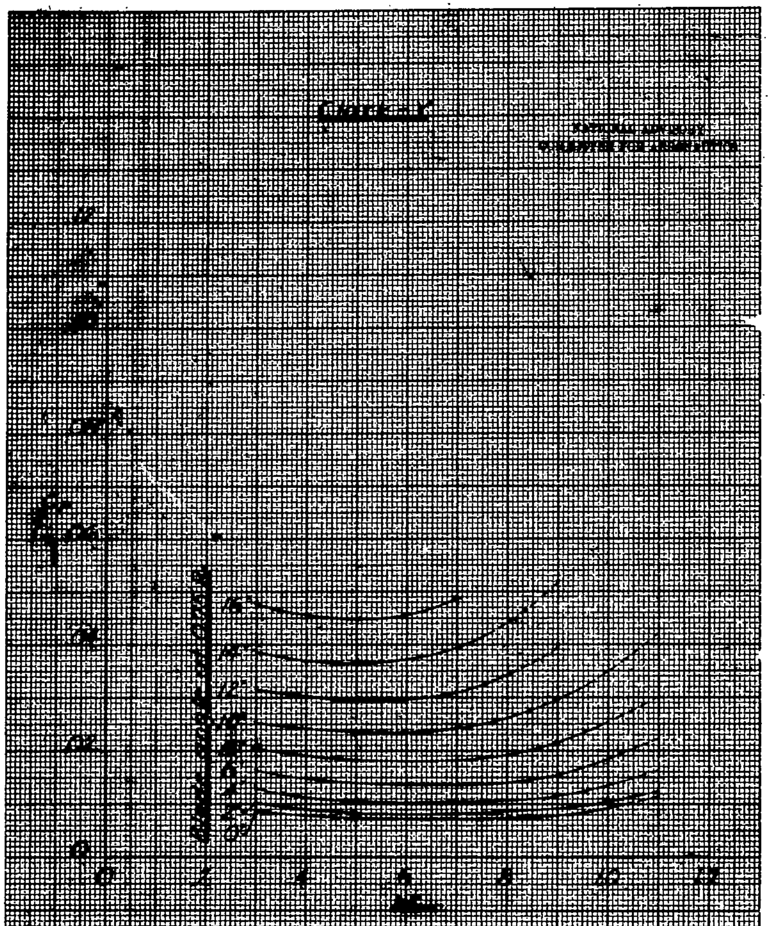

Figure [illegible].- Variation of static power coefficient with tip-speed ratio and blade angle. Two bladed propeller No. 69306-225.

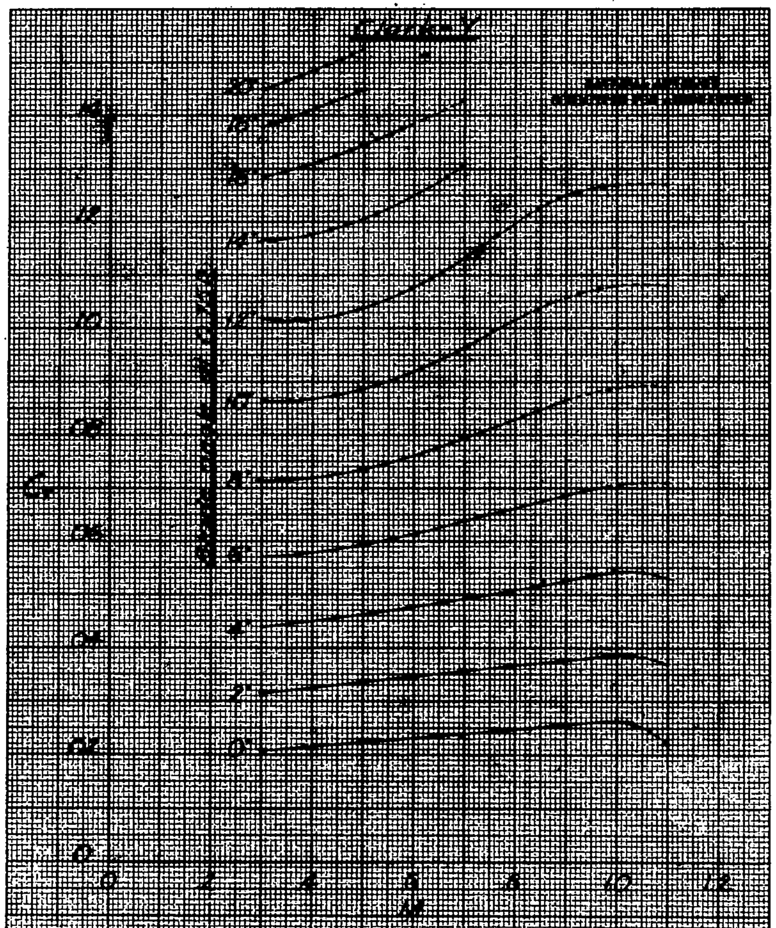

Figure 15.- Variation of static thrust coefficient with tip-speed ratio and blade angle. Three bladed propeller No. 69306-225.

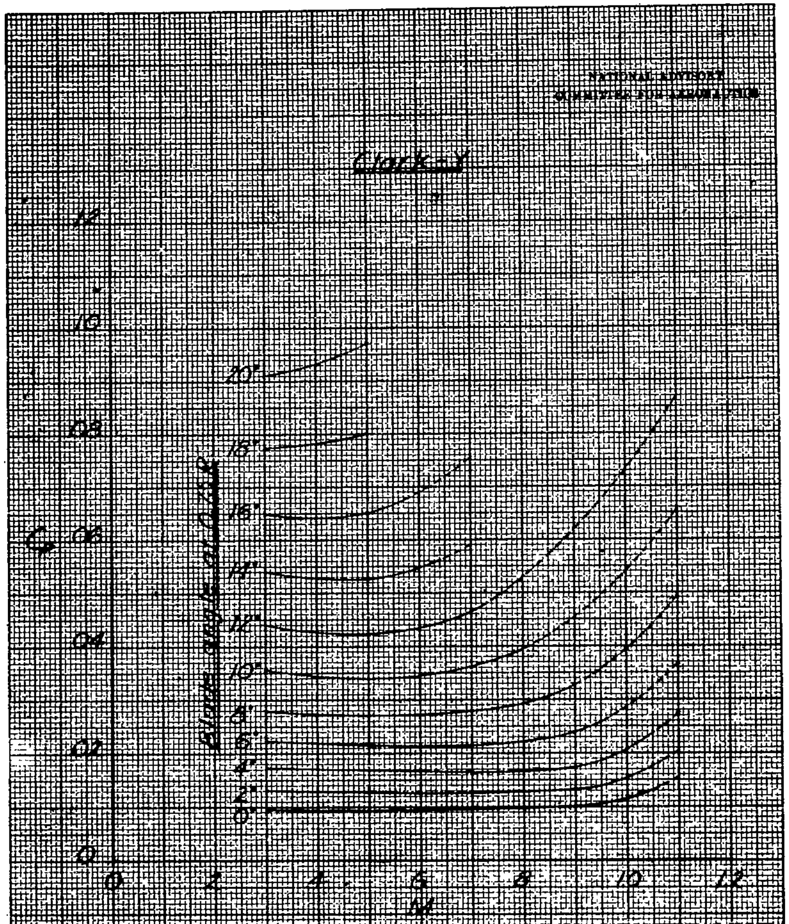

Figure 16. - Variation of static power coefficient with tip speed ratio and blade angle. Three bladed propeller No. 89806-225.

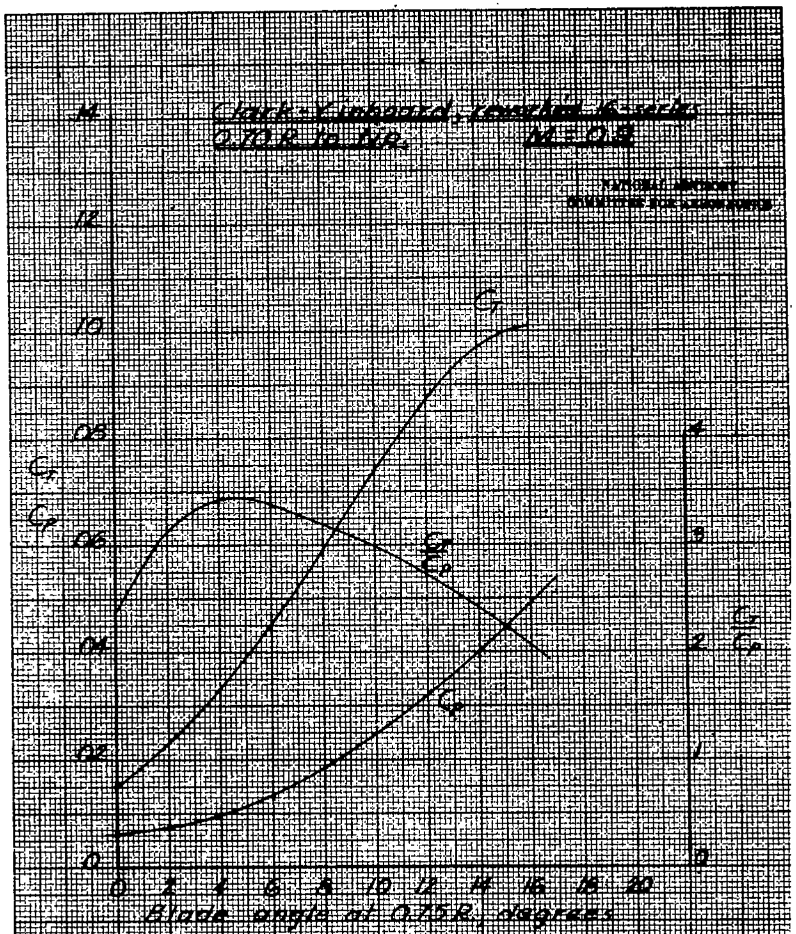

Figure 17. - Static propeller characteristics. Two bladed propeller No. 101392.

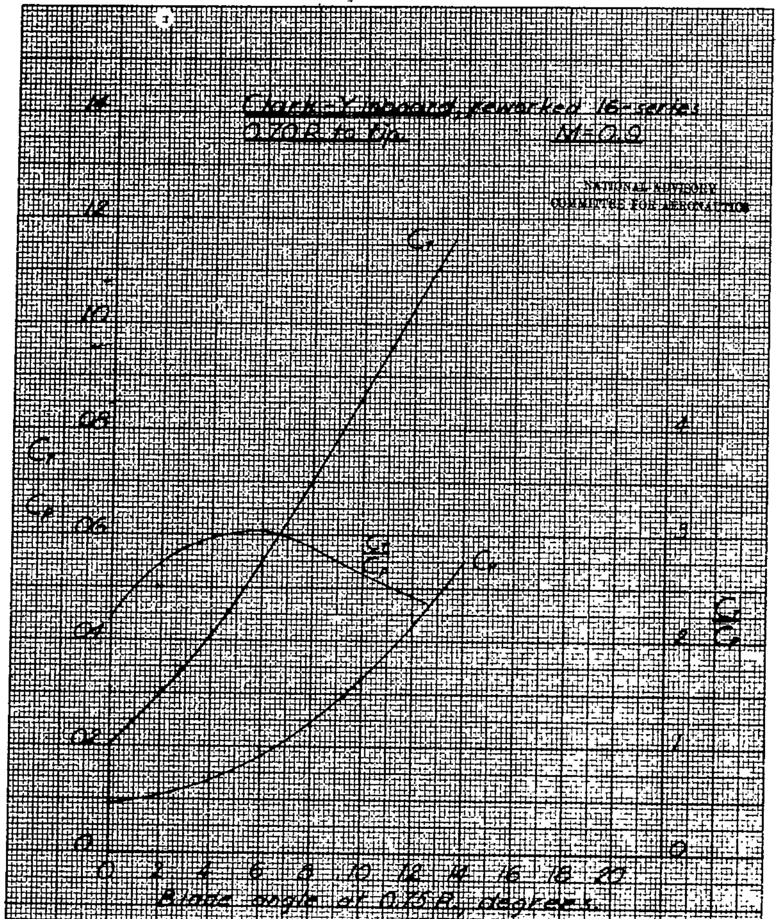

Figure 18. - Static propeller characteristics.
Three bladed propeller No. 101332

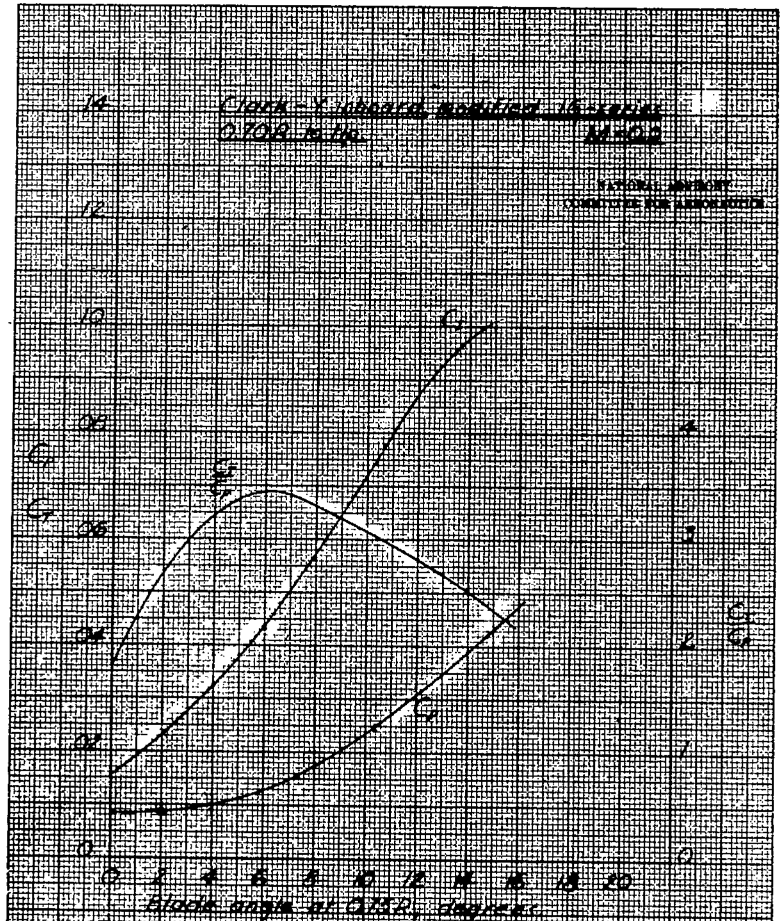

Figure 19. - Static propeller characteristics.
Two bladed propeller No. 101332

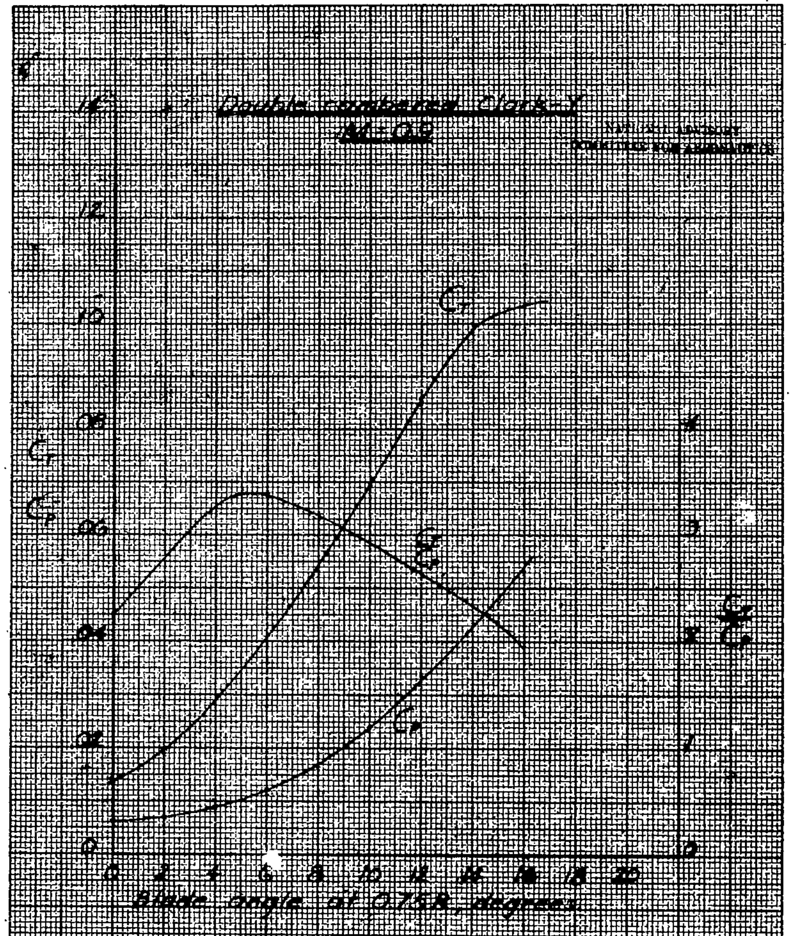

Figure 20.- Static propeller characteristics.
Two bladed propeller No. 101336.

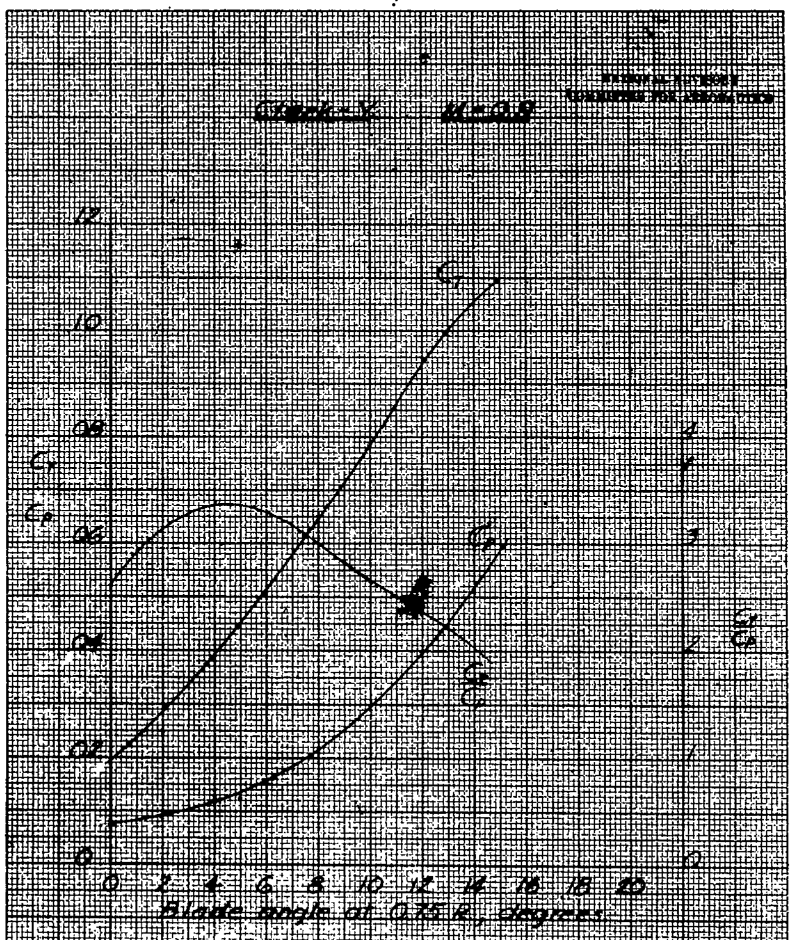

Figure 21.- Static propeller characteristics.
Two bladed propeller No. 89306-225.

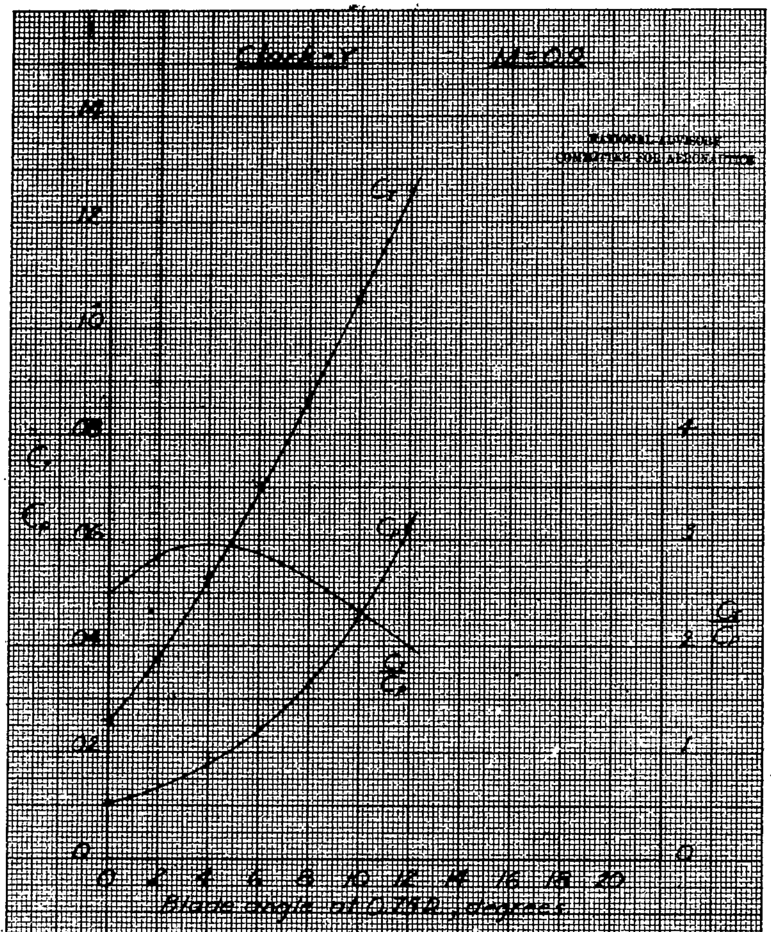

Figure 22.- Static propeller characteristics.
Three bladed propeller No. 89306-22S.

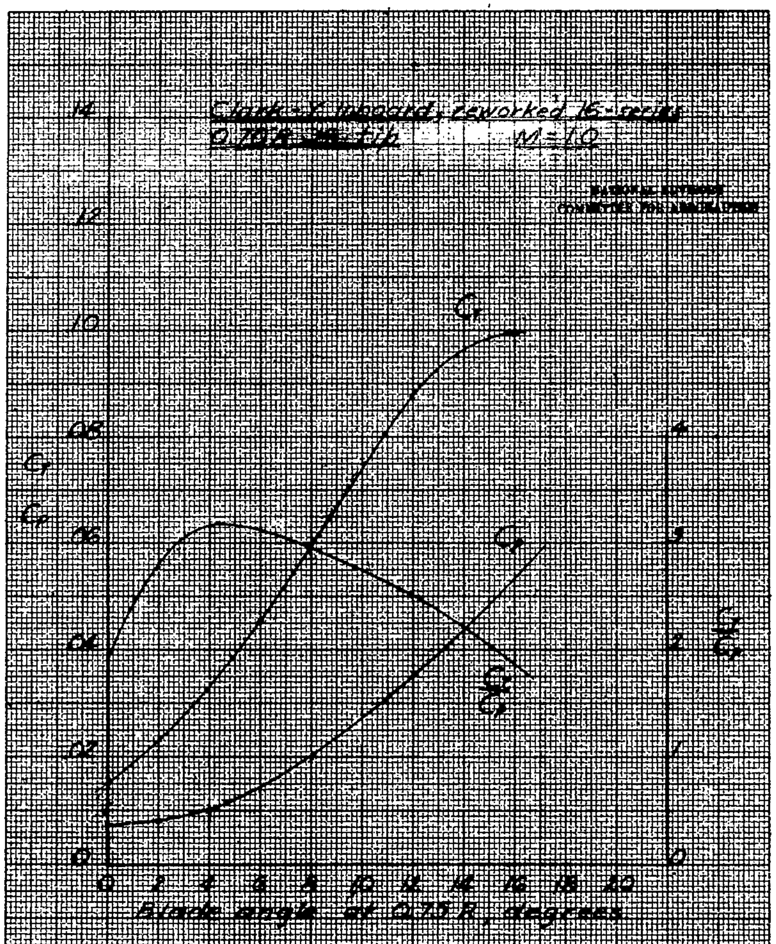

Figure 23.- Static propeller characteristics.
Two bladed propeller No. 101332.

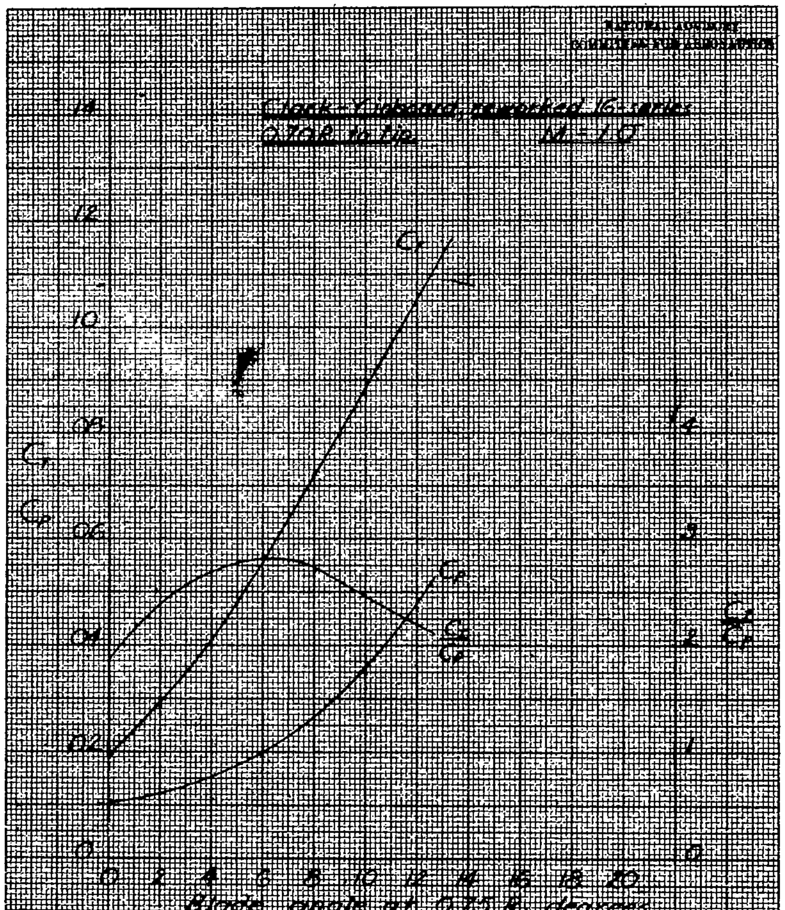

Figure 24.- Static propeller characteristics.
Three bladed propeller No. 101532.

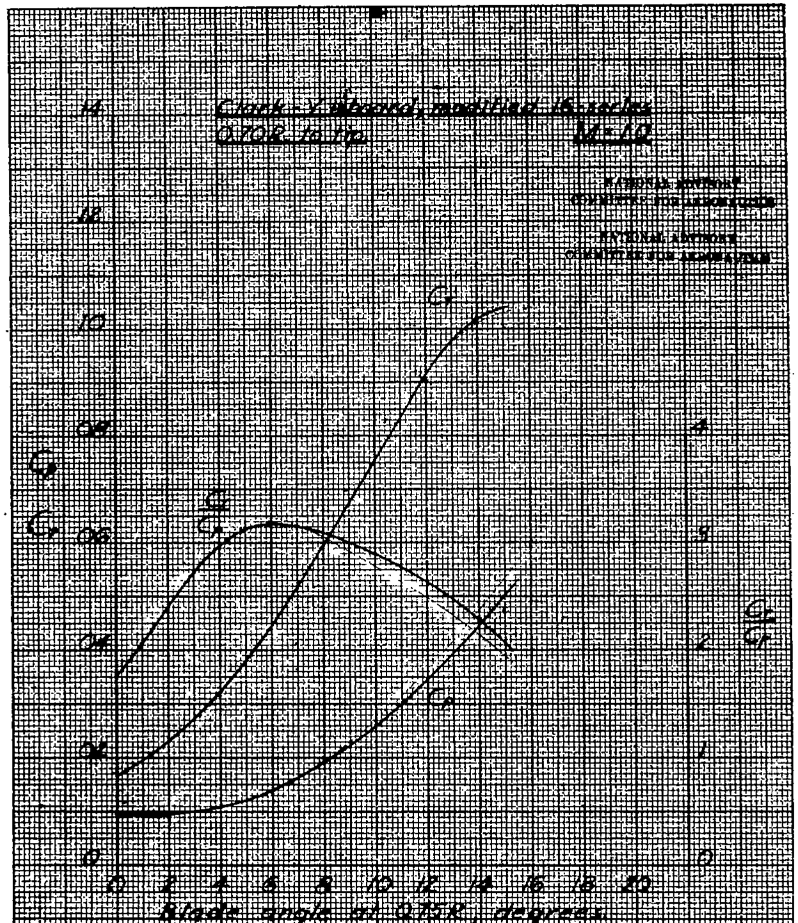

Figure 25.- Static propeller characteristics.
Two bladed propeller No. 101332.

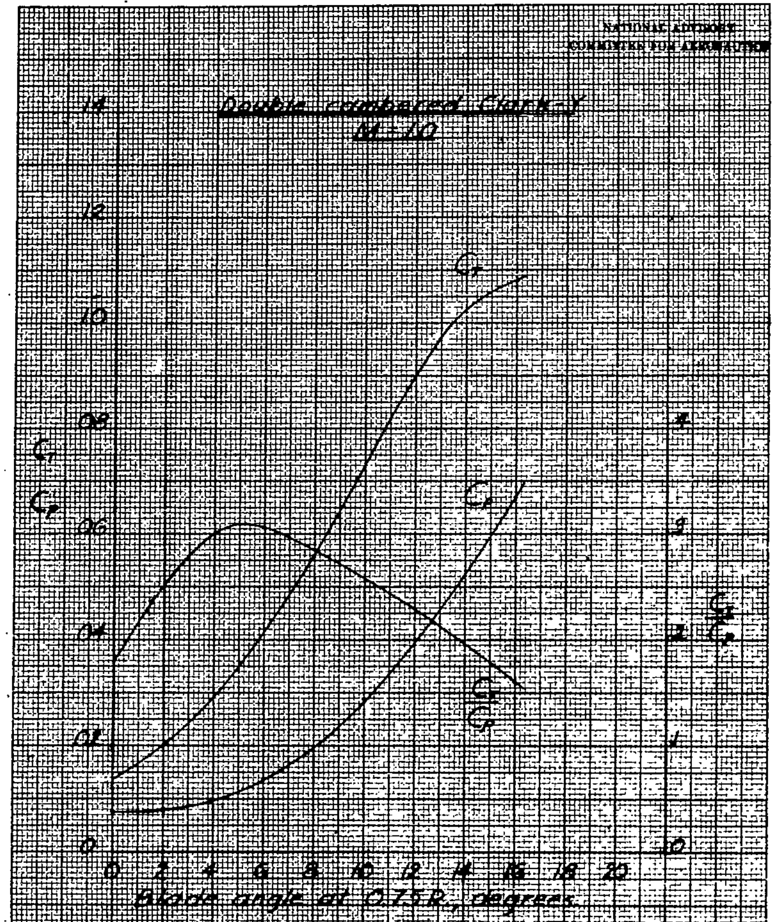

Figure 26.- Static propeller characteristics.
Two bladed propeller No. 101336.

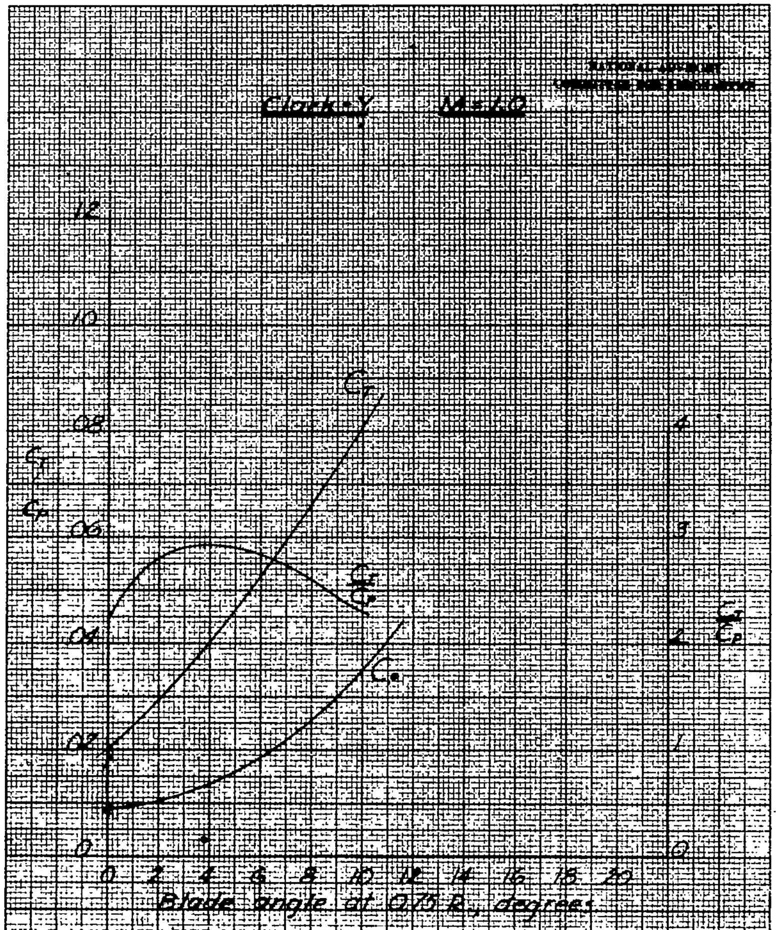

Figure 27.- Static propeller characteristics.
Two bladed propeller No. 89306-225

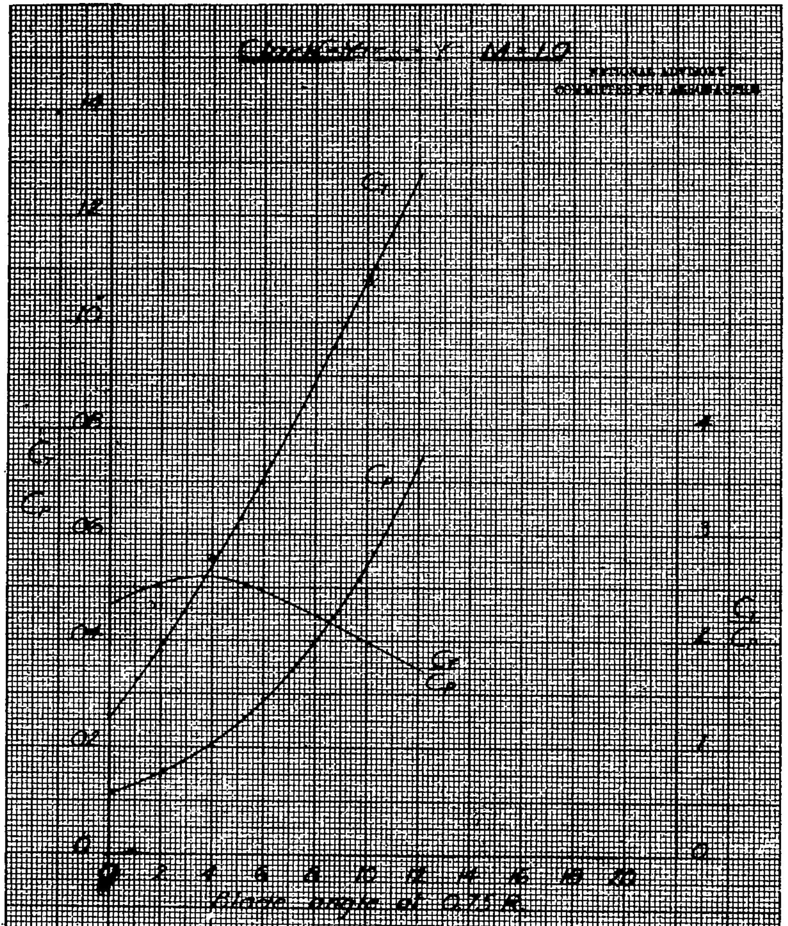

Figure 28.- Static propeller characteristics.
Three bladed propeller No. 89306-22.5.

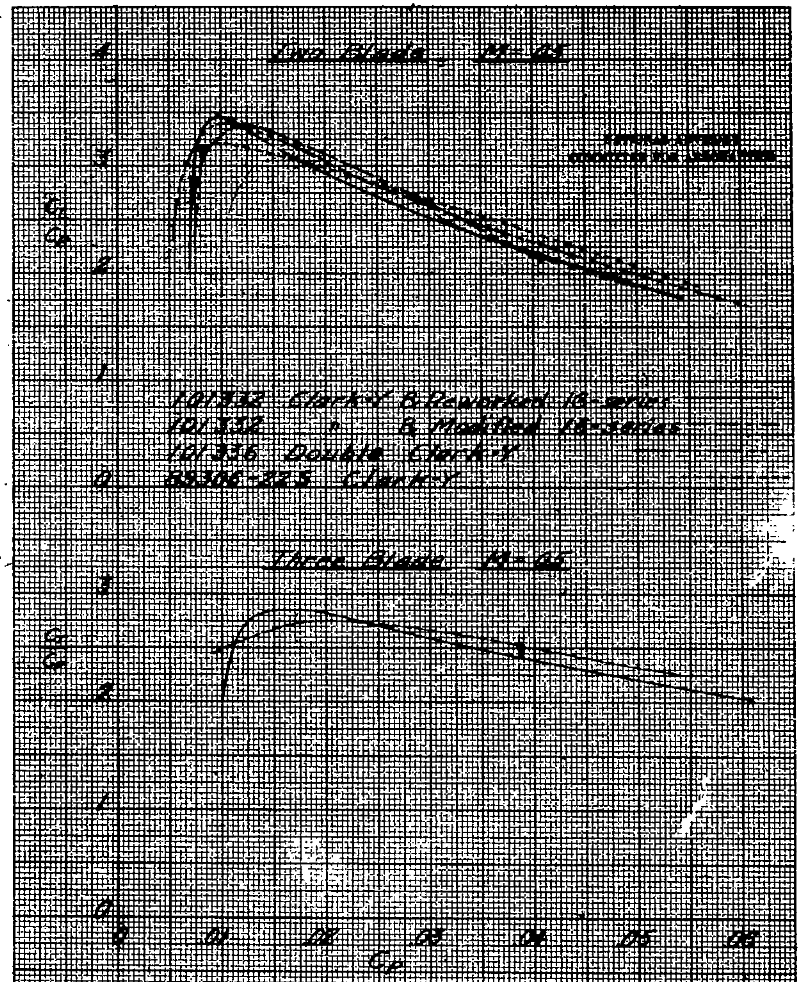

Figure 29.- Comparison of static thrust figure of merit.

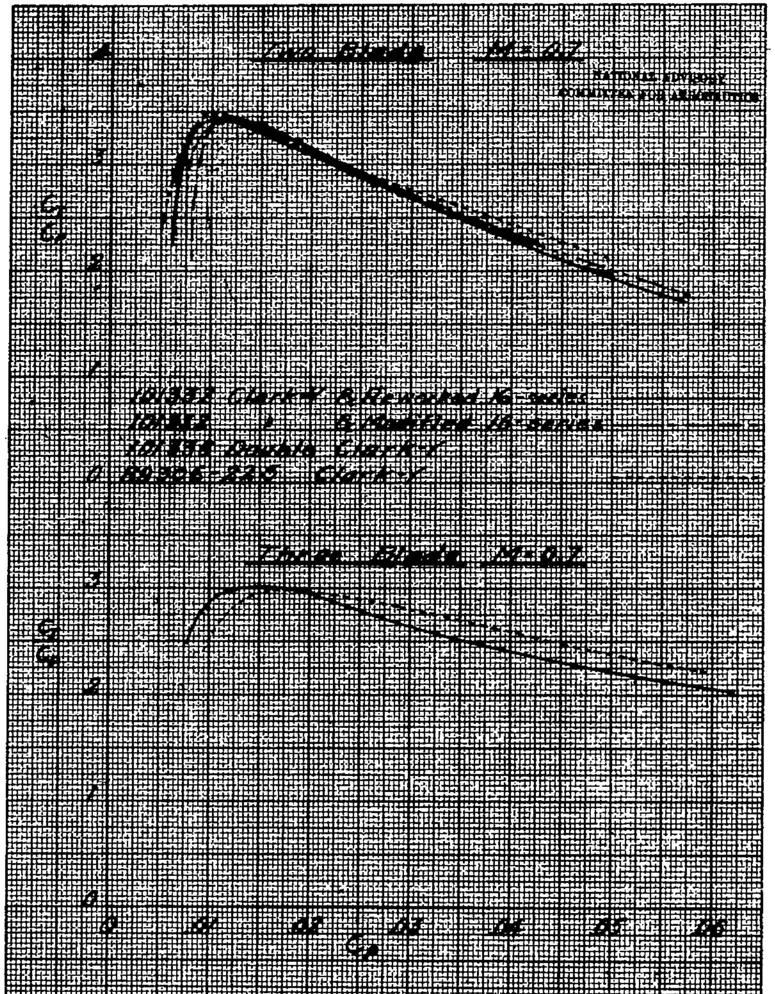

Figure 30.- Comparison of static thrust figure of merit.

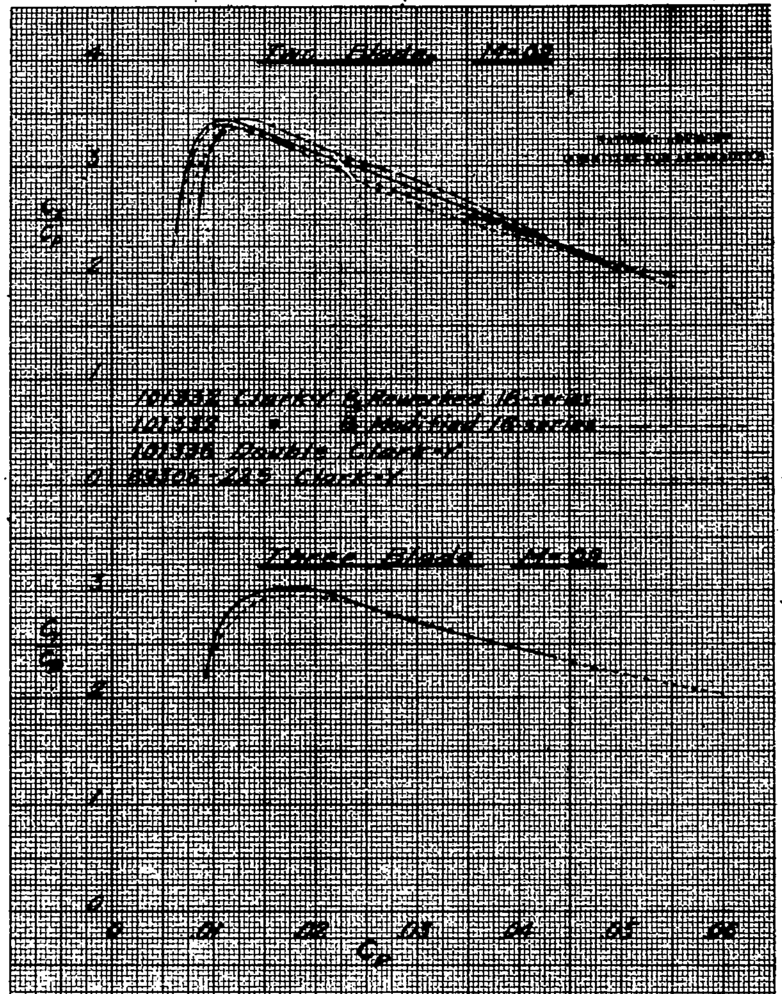

Figure 31.- Comparison of static thrust figure of merit.

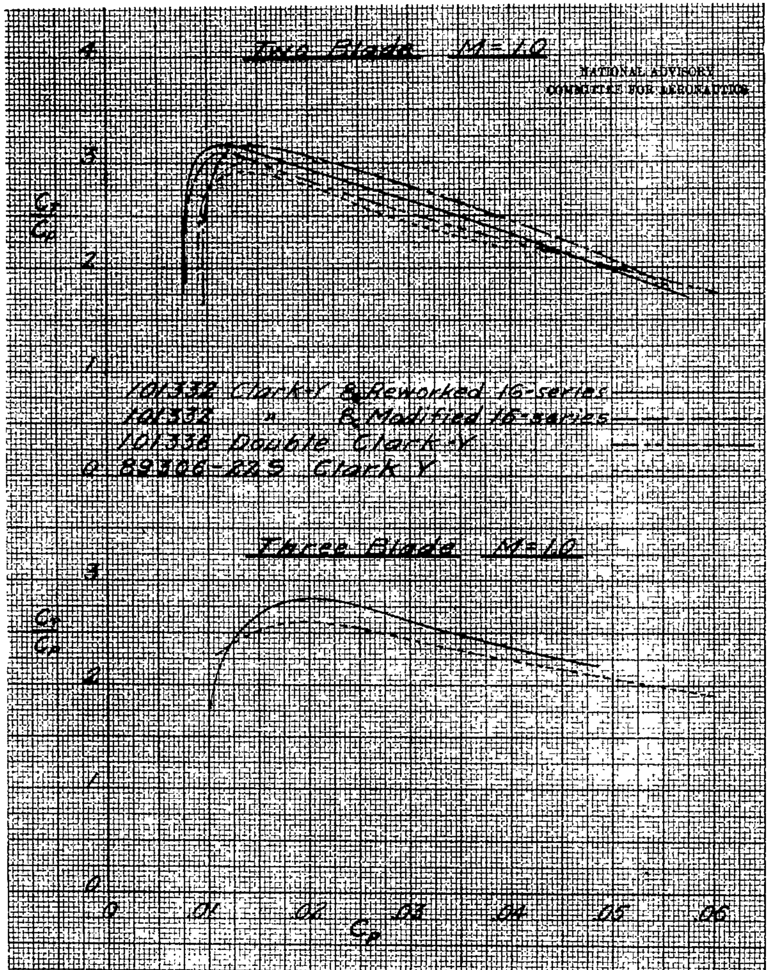

Figure 32.- Comparison of static thrust figure of merit.

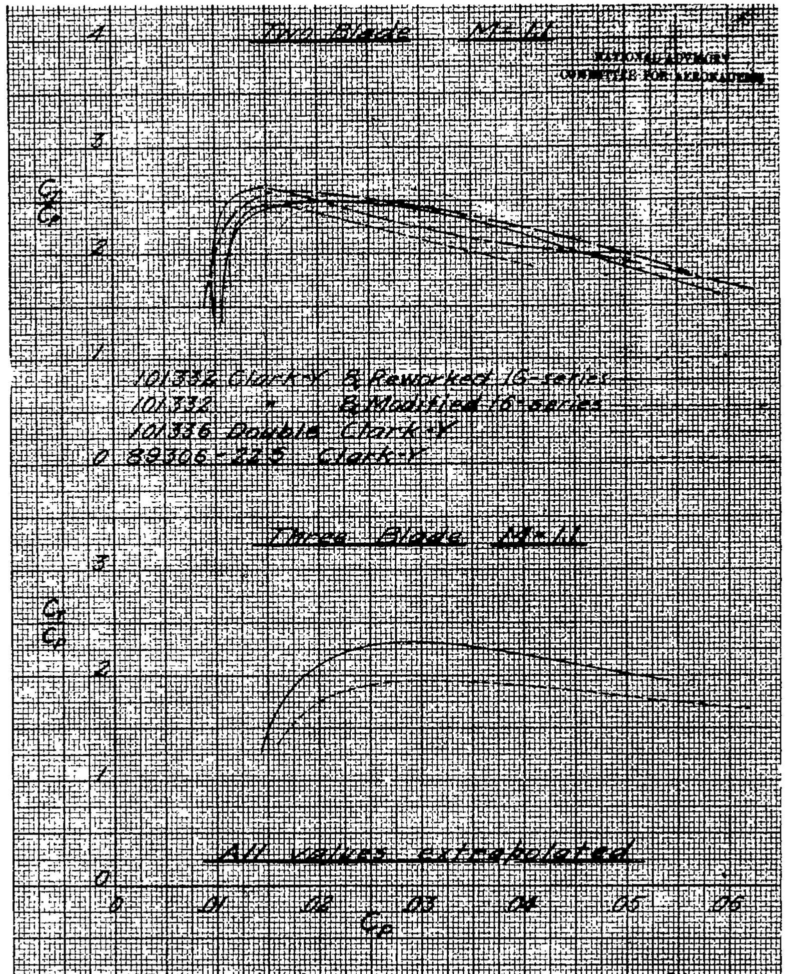

Figure 33.- Comparison of static thrust figure of merit.

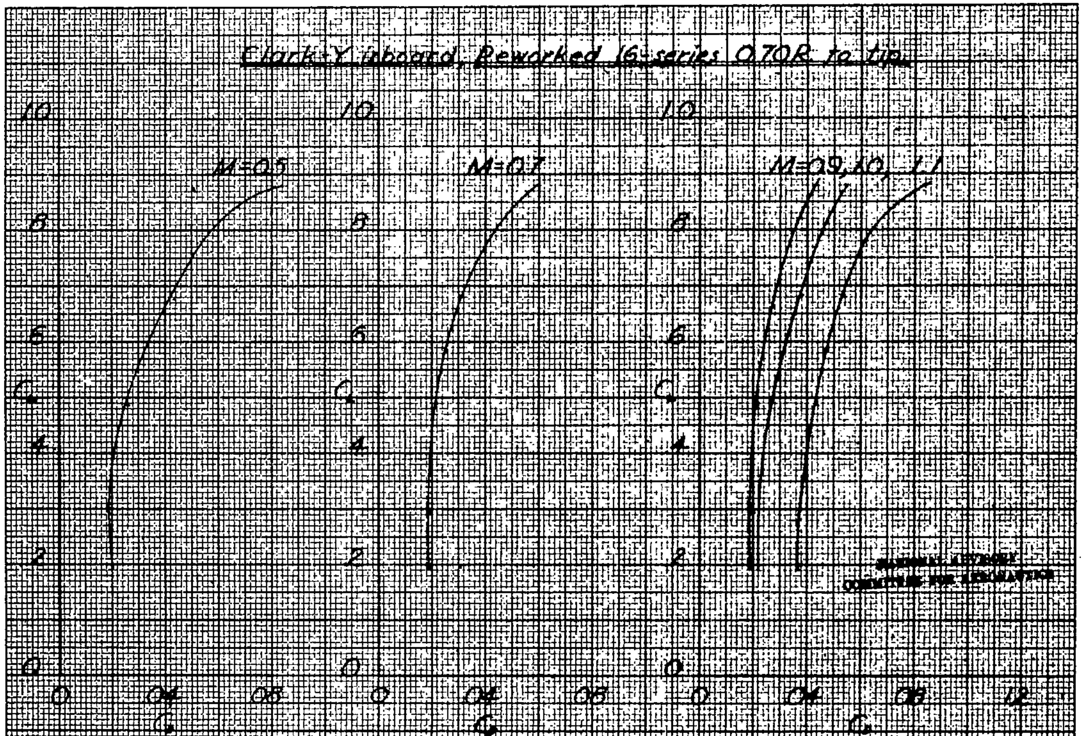

Figure 34.-Lift and drag coefficients computed from static propeller characteristics. Two bladed propeller No. 101532

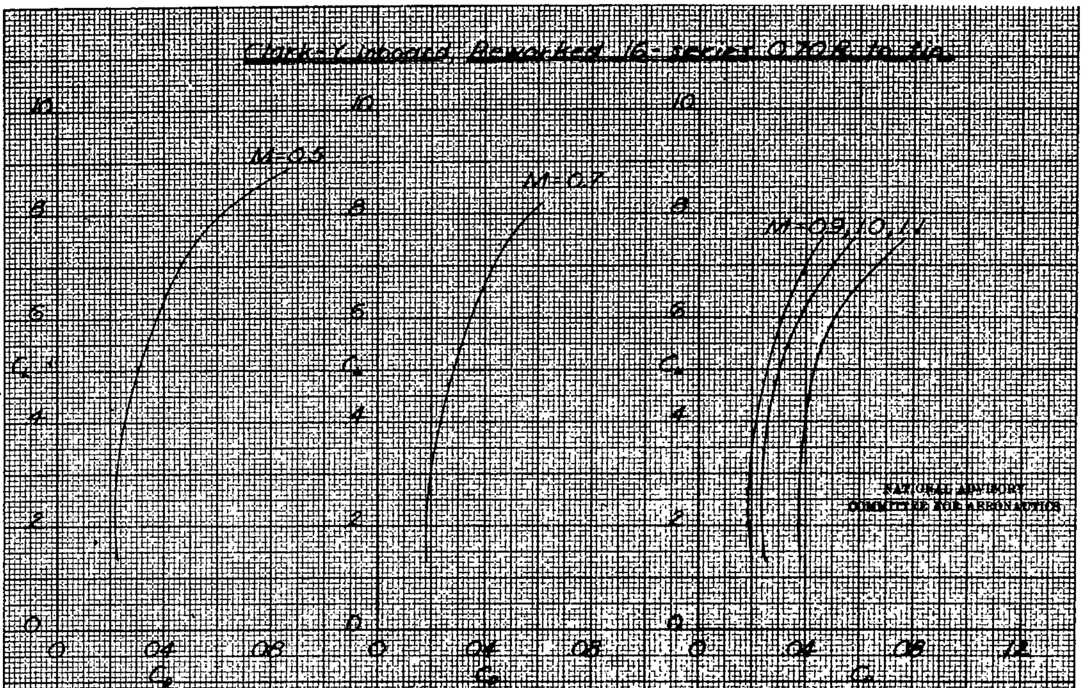

Figure 35.- Lift and drag coefficients computed from static propeller characteristics. Three bladed propeller No. 101332.

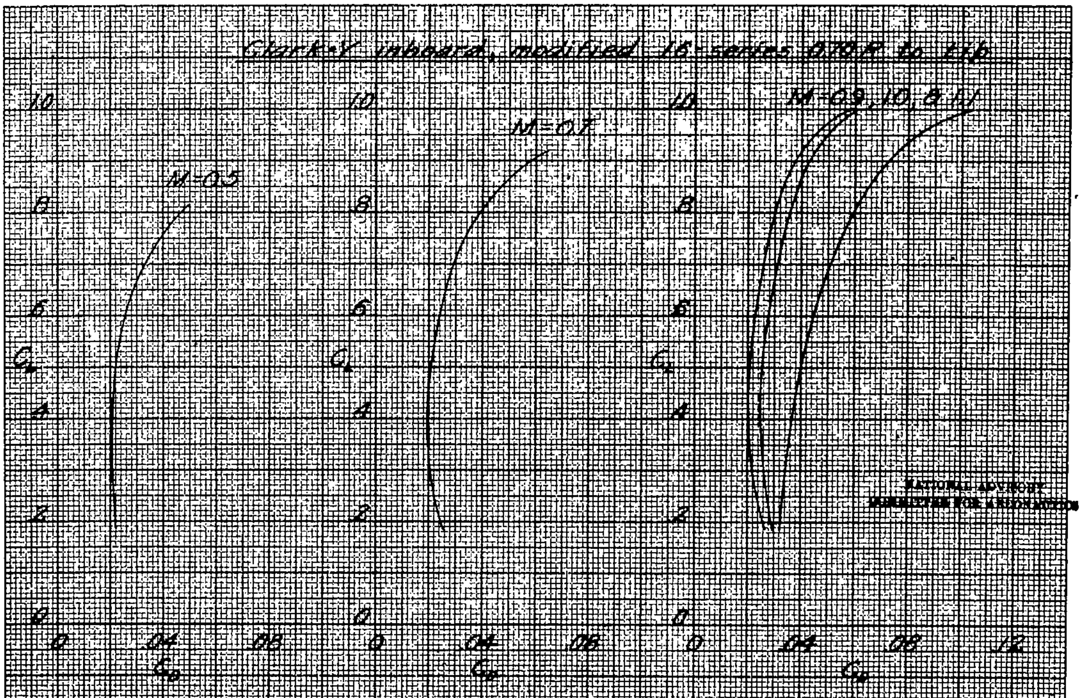

Figure 36.- Lift and drag coefficients computed from static propeller characteristics; two bladed propeller No. 101332.

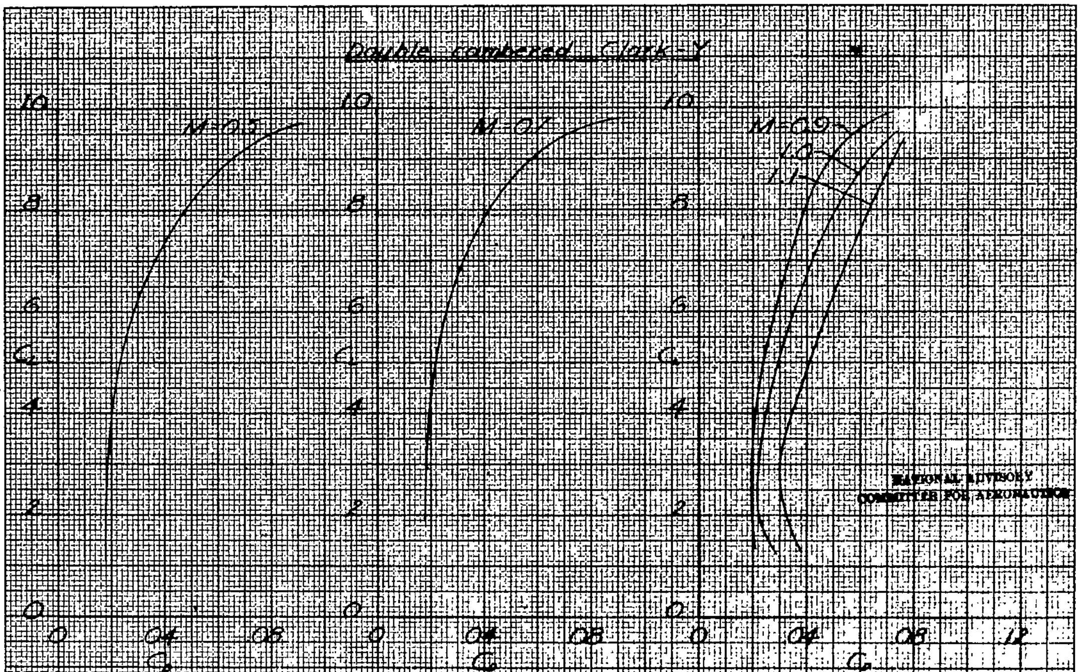

Figure 37.- Lift and drag coefficients computed from static propeller characteristics. Two bladed propeller No. 101336.

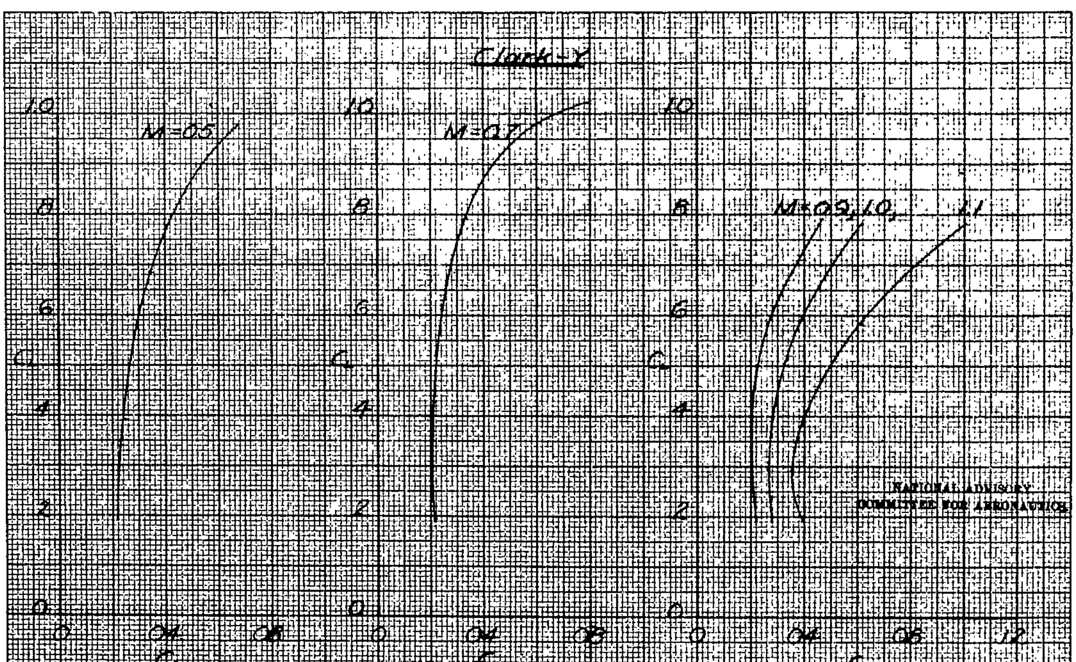

Figure 38.- Lift and drag coefficients computed from static propeller characteristics. Two bladed propeller No. B9306-2&5.

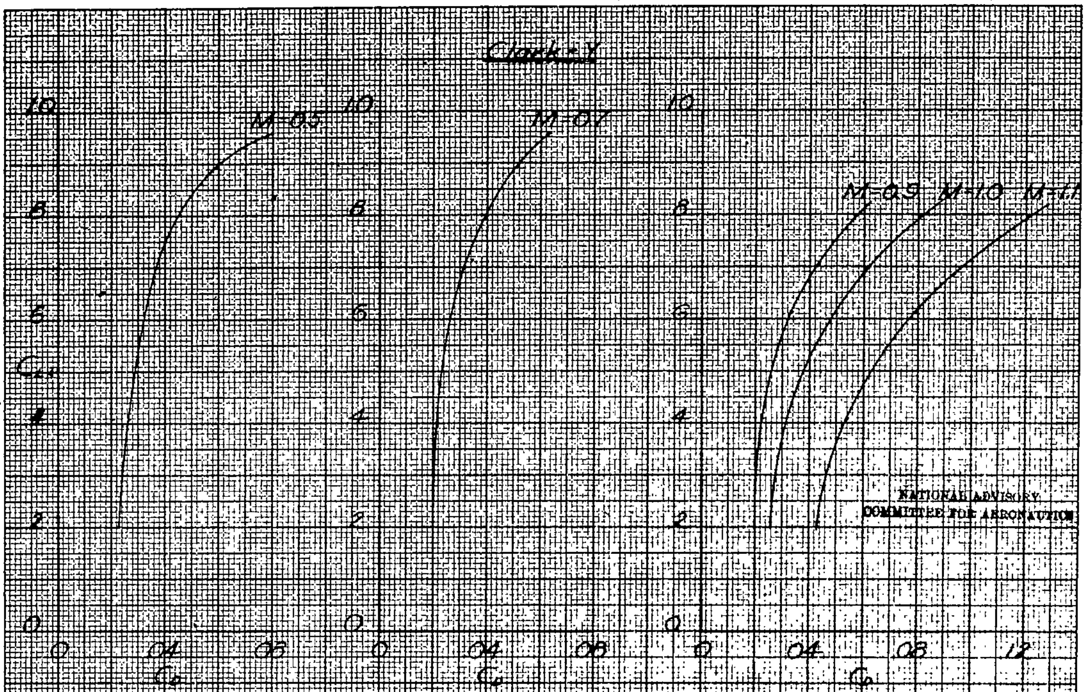

Figure 39. -Lift and drag coefficients computed from static propeller characteristics. Three bladed propeller No. 89306-225.

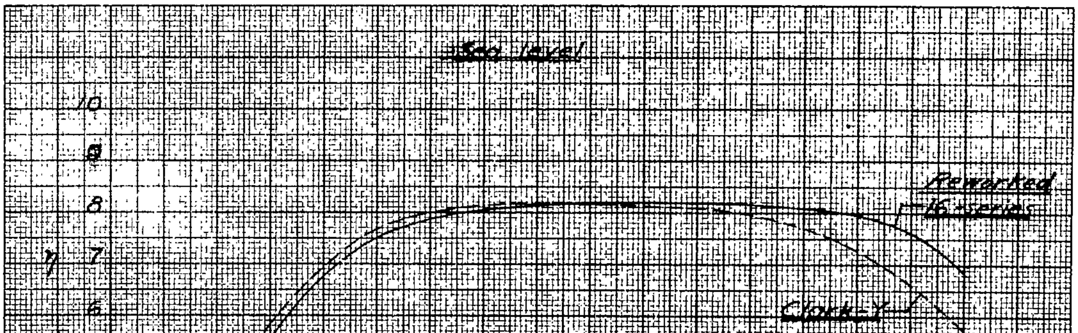

Figure 40.-Envelope efficiencies computed by Drigg's method; 2100 hp., 1500 propeller r.p.m., 10.55 ft. diameter three bladed constant speed propeller.